Burst firing in bee gustatory neurons prevents adaptation

Ashwin Miriyala, Sébastien Kessler, F. Claire Rind and Geraldine A. Wright*

Institute of Neuroscience, Newcastle University, Newcastle upon Tyne, NE1 7RU, UK
*author for correspondence, jeri.wright@ncl.ac.uk

Summary

Animals detect changes in the environment using modality-specific, peripheral sensory neurons. The insect gustatory system encodes tastant identity and concentration through the independent firing of gustatory receptor neurons (GRNs) that spike rapidly at stimulus onset and quickly adapt. Here, we show the first evidence that concentrated sugar evokes a temporally-structured, burst pattern of spiking involving two GRNs within the gustatory sensilla of bumblebees. Bursts of spikes resulted when a sucrose-activated GRN was inhibited by another GRN at a frequency of ~22 Hz during the first 1 s of stimulation. Pharmacological blockade of gap junctions abolished bursting, indicating that bee GRNs have electrical synapses that produce a temporal pattern of spikes when one GRN is activated by a sugar ligand. Bursting permitted bee GRNs to maintain a high rate of spiking and to exhibit the slowest rate of adaptation of any insect species. Feeding bout duration correlated with coherent bursting; only sugar concentrations that produced bursting evoked the bumblebee's feeding reflex. Volume of solution imbibed was a direct function of time in contact with food. We propose that gap junctions among GRNs enable a sustained rate of GRN spiking necessary to drive continuous feeding by the bee proboscis.

Keywords: coding, taste, gustatory receptor neuron, bursting, gap junction, adaptation, *Bombus terrestris*

Introduction

Sensory systems in animals have arrays of peripheral neurons where each individual neuron independently responds to the information that it perceives. Studies of the retina and the insect olfactory system indicate that in some cases, neighboring primary sensory neurons interact [1,2]. For example, a recent report from *Drosophila* showed that olfactory sensory neurons within the same sensillum mutually inhibit one another [2]. However, the generality and functional relevance of such interactions in the chemical senses remains obscure.

Gustatory sensory neurons in insects detect the identity and concentration of chemical compounds and translate information about them into action potentials (spikes). This encoding occurs in part through the specificity in receptor expression within the peripheral neurons [3–5], as well as through the rate and pattern of the spiking response [6–8]. In most insects, the dendrites of 2-4 gustatory receptor neurons (GRNs) are encapsulated within hair like sensilla [6], with each GRN expressing receptors that bind to tastants belonging to a specific taste category [3,9]. For example, in *Drosophila*, sugars like sucrose elicit spikes from a single 'sweet-responsive' GRN per sensillum that expresses several gustatory receptors sensitive to sugars [3,10]. GRNs that spike in response to stimulation with sugars typically increase their rate of firing as a function of stimulus concentration [11–14]. The pattern of the spike train is also thought to be relatively simple. In several insect species including *Drosophila*, individual sugar-sensing GRNs produce a brief increase in the rate of spiking during the first ~200 ms of stimulation that adapts rapidly to a tonic level with prolonged stimulation [6,10,15]. Deviations from this pattern are rare (but see [16] and [17]). Inhibitory interactions among GRNs have been reported only once before from the gustatory sensilla of insects [18].

Bee species collect and consume floral nectar: a solution composed mainly of sucrose, glucose and fructose [19]. Bee GRNs have only rarely been studied, and most studies are of honeybee GRNs. Here, we recorded from GRNs on the mouthparts of adult worker bumblebees (*Bombus terrestris)* to determine how sugar concentration is encoded. We found a novel, coherent temporal pattern of GRN activity characterized by bursts of rapid spiking that arise from gap junction-mediated inhibitory coupling between two GRNs within the same gustatory sensillum. This coupling affected GRN spike timing by reducing the rate of spike frequency adaptation during the first 1 s of stimulation. Burst firing in GRNs was a function of sugar concentration and depended on sugar identity. In contrast to other sensory

neurons and other insect GRNs, bursting bee GRNs maintained a high frequency of spiking during prolonged sugar stimulation, and only sugar concentrations that evoked bursting promoted robust feeding behavior. The burst structure was associated with a low variance in ISI, which increased exponentially as the GRNs adapted. When bees were allowed to feed, we found that the duration of their first feeding bout correlated with the period over which the structured burst spiking was observed (~7-10s).

Results

Concentrated sucrose evokes temporally structured, bursts of spikes involving two galeal GRNs

Bee species have a proboscis specialized for nectar collection and made of 5 parts: the paired galea, paired labial palps, and the glossa ([20], Figure 1 A). While all proboscis parts have gustatory sensilla, we focused our investigation on the most prominent, A-type sensilla of the galea (Figure 1 B). Cross-sections taken near the mid-point of an A-type sensillum revealed the dendrites of 4 GRNs (Figure 1 C). To measure the responses of these GRNs to tastant stimulation, we used an extracellular, two-channel recording method (i.e. tip-tungsten recording; see Methods). Surprisingly, stimulation of the A-type sensilla with 100 mM sucrose evoked a spiking response not seen in other insect GRNs. The sugar-sensing GRNs from these sensilla exhibited bursts of spikes riding on a low frequency oscillation (Figure 1 D). Both the spiking and oscillatory components of the response were restricted to the stimulation period (Figure S1 A-B).

We observed distinct spike waveforms (Figure 1 E) as well as superposition waveforms (Figure 1 F) that arise when multiple neurons fire within a small time-window coinciding with the absolute refractory period (i.e. within 2 ms). Using quantitative spike sorting techniques ([21,22], see Methods), we found that two GRNs were activated by sucrose stimulation, which we now refer to as GRN 1 and GRN 2 (1 s stim with 100 mM sucrose; Figure 1 E, F). GRN 1 fired at a rate of 81 ± 15 spikes/s, and GRN 2 fired with a slower rate of 17 ± 7 spikes/s (mean ± SD; n = 5 recordings, 5 animals). An average of 10 ± 4 superpositions of the GRN 1 and GRN 2 spike waveforms were detected for each recording.

The sucrose responsive GRNs were distinct from the mechanosensory neuron (Figure S1 C-D). Additionally, the burst response did not involve a water responsive GRN,

as a majority of the A-type sensilla (> 90%; 80 sensilla from 26 animals) did not evoke a spiking response when stimulated with distilled water. In contrast, B-type sensilla did possess a water responsive GRN, but it was silenced by the presence of sucrose at higher concentrations (Figure S1 E-F).

The positions of the GRN 1 and GRN 2 spikes were consistent within the burst structure: more than 95% of the bursts had a series of GRN 1 spikes within the bursts followed by a single GRN 2 spike or a superposition at the end of each burst (83/87 bursts, n=5 recordings, 5 animals; see methods, Figure S1 G for burst detection). Each burst had at least one spike from GRN 1 and one from GRN 2. A silent period of ~29 ± 7 ms followed the GRN 2 spike or superposition at the end of each burst. The frequency of the oscillatory component ranged from 17-27 Hz with an average of 22 $\pm$ 5 Hz (SD, n=5 recordings, 5 animals). GRN 1 fired near the peak of the oscillatory component with a mean phase of 17±72° (mean ± SD), and GRN 2 spikes were positioned on the negative slope with a mean phase of 83 ± 36° (Figure 1 G). The trough of the oscillation was consistent with the silent period between bursts. For all subsequently-presented un-sorted recordings, spikes within bursts will be assumed to be spikes from GRN 1 and spikes at the end of bursts from GRN 2.

Sensory input from the GRNs is integrated in the sub-esophageal zone (SEZ) of the insect brain. To verify that the bursting was transmitted downstream towards the SEZ, we made recordings from the axons of galeal GRNs in the maxillary nerve (MxN) while stimulating an A-type sensillum with 100 mM sucrose (Figure 2 A). Bursting activity and the oscillations from both classes of GRNs were transmitted along the axons (Figure 2 B). We also tested whether the burst structure arises from the activity of GRNs local to a specific sensillum. We used the tip recording technique to record and stimulate from the GRNs of two neighboring A-type sensilla while recording activity from the maxillary nerve (Figure 2 C). These recordings revealed that the activity of GRNs in different sensilla were not correlated (Figure 2 D), which indicates that GRN activity within a sensillum is independent of activity in neighboring sensilla.

Bursting could play a variety of roles in these neurons: it could affect the rate of adaptation to stimulation, it could be involved in coding the stimulus features (e.g. sugar identity and/or concentration), and it could potentially be important for coordinating mouthpart movement. We performed a series of experiments to investigate each of these potential functions in *B. terrestris* galeal GRNs.

Bursting GRNs are slow to adapt

Chemosensory neurons are often characterized by rapid spike frequency adaptation in response to prolonged stimulation [6,10,15]. In the bumblebee, the spike frequency of GRN 1 barely adapted during the first 2 s of stimulation with 100 mM sucrose; its ISI increased at a rate of only 3.3 $\pm$ 5.4 ms/s (median $\pm$ IQR; n=38 animals, 1 recording per animal; Figure 3 A). In comparison, the rate of adaptation of GRN 2 was 8x faster (25.8 ms/s).

Further, the adaptation rate of GRN 1 depended on GRN 2. When the spike frequency of GRN 2 was high (i.e. when GRN 2 had an ISI < 60 ms), the GRN 1 rate of spiking at the start of each burst *accelerated* (i.e. plots of ISI within each burst had a negative slope, Figure 3 B, C). An acceleration in spiking is the opposite of what would be expected if a GRN was adapting. The high frequency GRN 2 spiking and the associated acceleration of GRN 1 within bursts was observed within most recordings only during the first 0.8 s of stimulation (Figure 3 D). Over the course of prolonged stimulation, however, the spike frequency of both GRNs decreased (Figure 3 D,E). To investigate the adaptation dynamics of the GRNs, we stimulated the A-type sensilla with 100 mM sucrose for 30 s (Figure 3 E). As before, the initial portion of the response was characterized by the structured burst firing of both GRNs. As time progressed, the burst structure changed as the GRNs adapted. For recordings that exhibited strong, consistent bursting (>10 GRN 2 spikes in the first 1 s of stimulation), the spiking of both GRNs remained coherent for the first 7 s (low variance in ISI; Figure S2 A). After 7 s, the burst structure changed and the ISI variance increased exponentially.

Spike-time cross-correlation analysis revealed that the firing of GRN 1 was strongly inhibited by GRN 2 spikes for as long as 25 ms after GRN 2 fired (Figure 3 F). In addition, this analysis showed that GRN 1 spikes occurred with half of their expected frequency at 2 ms prior to each GRN 2 spike (Figure 3 F, Figure S2 B). Thus, the activity of GRN 1 strongly depends on the presence of a GRN 2 spike, and the activity of GRN 2 weakly depends on GRN 1.

The longer, 30 s recording revealed how the dynamic structure of the spiking of GRN 1 was affected by GRN 2. In recordings with strong bursting, the total rate of GRN 1 spiking increased over the first 0.8 s of the recording, reached a plateau, and then had a steady rate of decline of ~2 spikes/s for the period between 1-10 s of the recording (Figure 3 G, red trace). At 10 s into stimulation, the rate of adaptation of the GRN 1 slowed to ~0.3 spikes/s. By comparison, GRN 1 in recordings with little or no bursting (i.e. <10 GRN 2 spikes in the first 1 s of stimulation) exhibited a steady decline in firing up to 10 s (Figure 3 G, blue trace).

Thus, as we found previously, the rate of spiking – and hence the rate of adaptation of GRN 1 – depended on the activity of GRN 2. The burst structure dissolved as the both GRNs adapted to the stimulus.

Pharmacological blockade of gap junctions eliminates bursting

Our previous experiments indicate that GRN 1 and GRN 2 are coupled. Primary gustatory neurons do not have chemical synapses. However, the close proximity of the dendrites within the A-type sensilla (Figure 1 D) could make it possible for gap junctions to exist between the GRNs or could facilitate an ephaptic lateral interaction. For ephaptically-coupled neurons, the electric field associated with the spiking activity of one neuron alters the excitability of its neighboring neuron (e.g. [23]). It is unlikely that what we observe involves an ephaptic interaction, as such interactions are ~10 times shorter than the ~ 0.3 s inhibitory period we observed following the GRN 2 spike (Figure 3 F; [24,25]). On the other hand, ion flux through gap junctions has been shown to mediate transmission of long-duration, hyperpolarizing currents [26,27].

To test whether gap junctions could play a role in the interaction between GRN 1 and GRN 2, we exposed individual sensilla to the gap junction blocker, carbenoxolone (CBX, applied as carbenoxolone disodium salt; [28,29]; see Methods). After a 2 min exposure to 10 mM CBX, we found that the burst response was suppressed when stimulating with 100 mM sucrose (Figure 4 A,B). Spike sorting the traces revealed that GRN 2 ceased firing after exposure to CBX (Figure 4 C). Importantly, we found that the rate of adaptation of GRN 1 was significantly faster over the 5 s interval when GRN 2 was absent due to CBX knockdown (Figure 4 D, 2-way GLM, stimulus x interval, $\chi_8^2 = 30.5$, $P < 0.001$). This difference in the rate of adaptation was especially pronounced during the first 1 s of the recording (post-hoc lsd, Suc(initial) vs. CBX: $P < 0.001$; Suc(initial) vs. Suc(recovery): $P = 0.971$; CBX vs Suc (recovery): $P < 0.001$). The rate of adaptation changed substantially over the whole recording after exposure to CBX, but not for either stimulation with sucrose (Table S1).

The effect of CBX on the firing of GRN 2 was dose-dependent (Figure S3 A-B). We performed two sets of controls to confirm that the effect of CBX was due to its action on a gap junction and not on the gustatory receptor or due to the osmolarity of the solution (Figure S3 C-H). Mixtures of CBX in sucrose applied to the sensilla did not suppress the sugar-sensing GRNs (Figure S3 C-D) and did not activate a GRN in the first 1 s of stimulation (2 $\pm$ 2 spikes (mean $\pm$ SD), N=7 recordings, 7 animals). Further, 10 mM CBX did not affect the

initial firing rate of GRN 1 when stimulated with sucrose (Figure S3 E). However, prolonged exposure to 10 mM CBX did cause fluctuations in membrane potential and rapid spiking later in the recording, similar to that observed with exposure to quinine in other insects ([8,30]; Figure S3 F). Application of NaCl using the same protocol did not significantly influence the firing of GRN 2 between all three stimulation protocols, nor did it influence the rate of adaptation of GRN 1 (Figure S3 G,H). Thus, our data indicate that the bumblebee's GRNs are gap-junction coupled to produce a burst spiking response. These data are the first to indicate that burst firing is a mechanism that reduces the rate of adaptation in neurons.

Bursting bee GRNs have the slowest rate of adaptation of any insect

The coherent burst structure reported here for *B. terrestris* has not been observed in any other insect species. To observe whether this feature was common to bee species, we recorded from galeal mouthpart sensilla of the common carder bumblebee, *Bombus pascuorum*, the honeybee, *Apis mellifera*, the garden bumblebee *Bombus hortorum* and the red-tailed bumble bee *Bombus lapidarius* (Figure 5 A). These recordings demonstrated that bursting is a feature common to the proboscis GRNs of bee species.

Unlike bumblebee GRNs, most sugar-sensing GRNs in insects adapt rapidly from stimulus onset. We compared the rate of adaptation from the mouthpart GRNs of several insect species stimulated with sucrose (80-100 mM; Figure 5 B). Examples we could identify from the literature include the fruit fly (*D. melanogaster,* [31]), Mediterranean fruit fly (*C. capitata,* [32]), tobacco hornworm larva (*M. sexta,* [33]), blowfly (*P. regina,* [34]*),* cabbage white butterfly caterpillar (*P. brassicae*, [7]) and mosquitoes *(A. gambiae,* [14]; *A. aegypti*, [35]). The firing rate of sucrose-sensing GRNs in *Drosophila*, mosquito and tobacco hornworm larvae is high within the first 100 ms and drops or almost ceases spiking within 1 s of stimulus onset. The GRN 1 of bumblebees (*B. terrestris* and *B. pascuorum*) had the highest rate of firing (i.e., the shortest ISIs) over a 5 s period of stimulation. In these bee species, GRN 1 also had the lowest rate of adaptation over a 5 s interval (*B. terrestris*: 2.0 spikes/s; *B. pascuorum*: 1.3 spikes/s) of all the insect species we compared. Interestingly, recordings from GRNs of the honeybee galeal sensilla showed that they also exhibit a slow rate of adaptation (2.1 spikes/s), but honeybee galeal GRNs had a lower rate of spiking on average than the GRN 1 of *B. terrestris* or *B. pascuorum*. The bumblebees' GRNs and the honeybee's galeal GRNs are the only GRNs in Figure 5 B that exhibit bursting. Thus, we conclude that bursting in bee mouthparts GRNs is a mechanism for prolonged, rapid spike

firing when the sensilla are in contact with food.

Bursting is a function of sugar identity and concentration

To test the role of the burst pattern of spiking in concentration coding, we stimulated bumblebee A-type sensilla with a sucrose concentration series (Figure 6 A). The rate of spiking of GRN 1 and GRN 2 (and hence the bursting) during the first 1 s after stimulus onset was a function of sucrose concentration. Sucrose concentrations $\geq$ 5 mM produced spikes from GRN 1. When the sucrose concentration was $\geq$ 10 mM, GRN 2 started firing and we began to observe bursts in the spike trains (blue traces in Figure 6 C, D, see Methods for model fitting).

The monosaccharides, fructose and glucose, are also important constituents of floral nectar. Like sucrose, fructose and glucose evoked bursting (Figure 6 B), but they did so at different threshold concentrations (GRN 1: Figure 6 C, Table S2, $F_6 = 65.5$, $P < 0.001$; GRN 2, Figure 6 D, Supplementary Table 3, $F_6=14.5$, $P < 0.001$; see methods for model fitting and comparison). A comparison of the EC_{50} values (i.e. threshold concentration that elicits spiking) between the three sugars for the GRN 1 revealed that sucrose was the best ligand at low concentrations (Tables S2). At higher concentrations when the GRN 2 spiking rate reached its asymptote, fructose evoked the highest spiking rate followed by sucrose and then glucose (Table S3).

Higher concentrations of each of the ligands were required to activate GRN 2 than GRN 1 (Figure 6 C,D). GRN 2 had a lower threshold for detection of sucrose and fructose than for glucose (Table S3) and reached an asymptotic rate of spiking above 100 mM. At the asymptote, sucrose and fructose evoked a higher spiking rate from GRN 2 than glucose (Table S3, glucose average firing rate was only ~5 spikes/s at 100 mM glucose and ~8 spikes/s at 1000 mM). The difference in threshold and asymptote for GRN 1 and GRN 2 indicates that each is likely to house gustatory receptors with different sensitivities to sucrose, fructose, and glucose. Thus, activation of each neuron and burst patterns of spikes in these GRNs depends on both the concentration of the sugar stimulus and its identity.

Galeal GRN sensitivity to nectar sugars is reflected in the dynamics of feeding behavior

One of the main functions of GRN input is to drive motor neurons that control feeding behaviors. To understand which features of the GRN activity were correlated with behavior, we tested how stimulation of the bumblebee's mouthparts with sucrose, fructose, and

glucose affected the initiation and continuation of feeding. We first used an assay where stimulating the proboscis elicits the proboscis extension response (PER) to study feeding initiation (see Methods).

On average, the PER was initiated within the first 1 s after stimulation (Figure 6 E, top). The probability of producing the PER increased with concentration (Figure 6 E, bottom; GLM, $\chi_4^2 = 51.4$, $p < 0.001$) and depended on the sugar used to stimulate the bee (GLM, $\chi_2^2 = 5.83$, $p= 0.054$). In general, fructose and sucrose were the most likely to produce the PER, and stimulation with fructose and sucrose elicited the PER at lower concentrations than glucose (least squares difference, all $p< 0.050$). Thus, only concentrations that produce robust bursting in GRNs also evoke feeding initiation in bumblebees.

After the mouthparts contact a food source, the GRNs continue to instruct the neural circuits involved in feeding. We tested how stimulus identity and concentration affected the volume of food ingested and the structure of feeding behaviour of bumblebees ([36]; see Methods). The duration of the first feeding bout (i.e. first continuous contact of the mouthparts with the solution) increased as a function of sucrose concentration (Figure 6 F, Figure S4 A; GLM, $\chi_5^2 = 77.0$, $P < 0.001$). Bees tested with 100 mM sucrose solution stayed in contact with the solution for an average 8.4 $\pm$ 5 s; the first bout duration of bees tested with the 1000 mM sucrose solution lasted ~27 s (Figure 6 F, Figure S4 A). The number of contacts the bees made with the solution also increased as a function of concentration (Figure S4 B; GLM, $\chi_5^2 = 22.8$, $P < 0.001$). Concentration-induced changes in feeding structure (first bout duration and the number of feeding bouts) occurred for all three of the sugars we tested (first bout: GLM, $\chi_2^2 = 3.38$, $P = 0.184$; no. bouts: GLM, $\chi_2^2 = 0.499$, $P = 0.799$).

Longer bouts of food contact also resulted in more food consumed (Figure 6 F, Figure S4 C, linear regression, $R^2 = 0.579$, $t = 8.73$, $P < 0.001$). Bees ate more of the high concentrations of the sugar solutions during the observation period (Figure 6 F, Figure S4 D, linear regression $t = 3.49$, $P = 0.001$), and they ate more sucrose and fructose than glucose (linear regression, $t = -4.35$, $P < 0.001$). Thus, our data indicate that the sugars and concentrations that cause bursting also produce longer bouts of contact with solutions, permitting the bee to obtain more food.

Discussion

Resistance to adaptation through gap junction mediated inhibitory interactions

Lateral inhibition of one peripheral chemosensory neuron by another is likely to contribute to information coding. In *Drosophila,* olfactory sensory neurons responding to different monomolecular ligands exhibit lateral inhibitory interactions [23]. The activity of one neuron silenced the other only when it was stimulated with its specific ligand [23]. Through mutual inhibition, the rate of activation of the two olfactory neurons signaled information about the relative proportion of two ligands in an olfactory stimulus. In contrast, our data are the first to demonstrate that inhibition of one GRN by another produces a distinct bursting pattern of spikes that involves both neurons. Our data show that periodic inhibition of GRN 1 by GRN 2 permitted GRN 1 to maintain a high, average rate of spiking over a longer period. Coherent bursts of spikes only occurred at concentrations of sucrose, fructose and glucose that elicited feeding behavior.

Burst firing has previously been defined as two or more spikes followed by a period of inhibition that results from mechanisms intrinsic to a neuron [37,38] or from synaptic input from a neighboring neuron [39,40]. Here, we show that peripheral chemosensory neurons burst as a result of interactions facilitated through gap junctions. Bursting in these neurons occurred when single GRN 2 spike inhibited the ligand-dependent activity of GRN 1 for a period of up to 25 ms. By comparing the rate of adaptation of GRN 1 in the absence or presence of GRN 2 spikes, we found that bursting reduced the rate of adaptation in GRN 1, especially during the first 1 s of stimulation with 100 mM sucrose. These are the first data we know of that show that bursting is a mechanism that allows neurons to maintain high rates of firing.

Our data indicate that the temporal pattern of spiking that characterizes bursts in bee GRNs is mediated by gap junctions. Gap junctions facilitate the bidirectional movement of ions and metabolites, permitting one neuron to alter the potential of its joined neighbors [41]. When we blocked electrical synapses and then stimulated with 100 mM sucrose, we observed that GRN 1 spiked but GRN 2 did not. The inhibitory period that defined the bursts was also suppressed. This provides further evidence that bursts of spikes occur as a result of the hyperpolarizing potential associated with spikes from GRN 2. The asymmetric inhibition of GRN 2 by GRN 1 probably indicates that the current flow facilitated by the gap junction is rectified due to differential resistance of each neuron, as observed in the crawfish and fruit fly giant fiber systems [41–43].

Bursting in GRNs correlates with sugar metabolic value

In insects, GRNs synapse onto interneurons in the sub-esophageal zone (SEZ).

Signals impinging on this network affect the balance of excitation and inhibition and coordinate the activity of motor neurons that generate proboscis extension and ingestion [44]. Our experiments clearly show that within the first 1 s of stimulation, the high concentrations that elicit bursting in the GRNs also initiate feeding. We note that the threshold for the production of bursting was 5-10 x lower than the concentration needed to evoke the PER. For this reason, we expect that responses from GRNs distributed across the mouthparts are necessary to elicit the PER [17].

While all three sugars we tested have metabolic value to bumblebees, sucrose has twice the value of either fructose or glucose, so it is perhaps unsurprising that its threshold for detection was lowest. Fructose at high concentrations evoked the most spikes and bursts and was most likely to elicit the PER. Fructose has additional value to bumblebees because it is used as a metabolic substrate by the flight muscles to produce shivering when bumblebees experience cold temperatures [45]. Bumblebees may also store energy in the form of haemolymph fructose [46]. The difference in the GRN responses to these three sugars could indicate that bees have evolved to code sugar identity through the burst activity of their GRNs.

Bursting: a mechanism to resist adaptation and maintain continuous feeding

In the insect gustatory system, one of the main functions of GRN input is to drive feeding behaviour [6,47]. When GRNs adapt, this could slow or stop the motor program of the mouthparts and cause an insect to remove its mouthparts from food. Moving sensilla in and out of contact with food substrates would be a way to repeatedly sample in order to be selective about food intake. For example, adult *Drosophila* feed on complex substrates composed of many compounds both toxic and nutritious. When feeding on sucrose, fruit flies repeatedly take little sips of 130-160 ms long with an interval of 80 ms between each sip [48]. The fly proboscis rarely remains in contact with the substrate for longer than 200 ms [48]. Strikingly, a single GRN in each mouthparts' sensilla of *Drosophila* fires rapidly for the first 100-150 ms of stimulation with sucrose, and then adapts to a steady state of firing by 200 ms during prolonged stimulation (Figure 5, [31]). Fly GRN periods of brief but high rates of firing followed by rapid adaptation therefore strongly correlate with the structure of proboscis contact with food.

A correlation between GRN firing rate and food contact duration was also evident in our data. Bee galeal GRNs maintain a high rate of firing due to coherent bursting; this is especially apparent in the first 1 s of stimulation, but is maintained for up to during 7-10 s of

stimulation with 100 mM sucrose. As in flies, the mean duration of the first bout of continuous contact with 100 mM sucrose was directly correlated to this time interval (mean = 8 ± 5 s). In contrast to flies, bee GRNs maintain a high rate of firing and their mouthparts stay in contact with food for ~60x longer during their first feeding bout. Through this comparison with *Drosophila*, we conclude that the high rates of GRN spiking that occur when bee GRNs burst makes it possible for bees to maintain contact with food during feeding. Bees drink floral nectar which is mainly composed of concentrated sucrose, glucose, and fructose. In a 2 min observation period, bees make few contacts with food (~2-3x) but can consume as much as 45-50 µl of sugar solution. Perhaps, acquiring food quickly through continuous feeding is most important for bees, as they compete with other pollinators for access to floral resources.

Our data clearly show that the sustained rate of firing was due to the burst structure caused by the interaction of the two GRNs and that this mechanism is common to other bee species. This is the first report we know of where bursting in neurons of any kind functions as a mechanism to resist adaptation. The way that GRN input is assembled by the SEZ to control the proboscis is slowly being revealed using models like *Drosophila*. Among insects, bees have the fewest genes for gustatory receptors [49].

Our data show that bees have unique mechanisms for encoding gustatory information. Identifying the limits of the bee gustatory system may reveal insights into the gustatory code unavailable in other model organisms.

Acknowledgements: The authors would like to thank Mark Stopfer, Yu-Shan Hung, Fabrizio Gabbiani, Joby Joseph and Scott Waddell for their comments on the manuscript; Zane Aldworth for help with spike sorting; Electron Microscopy Research Services at Newcastle University for help preparing the SEM photographs; Hauke Koch and Phil Stevenson for supplying *B. pascuorum* workers; and Carolyn Ma, Alex Simpson, and Marta Barberis for help with the behavioural data collection. This work was funded by the Leverhulme Trust (RPG-2012-708) and a BBSRC grant (BB/M00709X/1) to GAW and a Newcastle University Overseas Research Scholarship to AM.

Author Contributions: AM, SK, and GAW designed the experiments and analysed the data. AM and SK performed the electrophysiology and behavioural experiments. CR advised on histological methods and TEM images. AM, SK, and GAW wrote the manuscript.

Declaration of Interests: The authors declare no competing interests.

References

1. Shaw, S.R. (1975). Retinal resistance barriers and electrical lateral inhibition. Nature *255*, 480–483.
2. Su, C.-Y., Menuz, K., Reisert, J., and Carlson, J.R. (2012). Non-synaptic inhibition between grouped neurons in an olfactory circuit. Nature *492*, 66–71.
3. Thorne, N., Chromey, C., Bray, S., and Amrein, H. (2004). Taste perception and coding in *Drosophila*. Current Biology *14*, 1065–1079.
4. Thorne, N., and Amrein, H. (2008). Atypical expression of *Drosophila* gustatory receptor genes in sensory and central neurons. Journal of Comparative Neurology *568*, 548–568.
5. Weiss, L.A., Dahanukar, A., Kwon, J.Y., Banerjee, D., and Carlson, J.R. (2011). The molecular and cellular basis of bitter taste in *Drosophila*. Neuron *69*, 258–272.
6. Dethier, V. (1967). The Hungry Fly: A physiological study of the behavior associated with feeding. pp. 64–72 (Cambridge, UK: Harvard Press)
7. Schoonhoven, L.M., and Van Loon, J.J.A. (2002). An inventory of taste in caterpillars: Each species its own key. Acta Zoologica Academiae Scientiarum Hungaricae *48*, 215–263.
8. Glendinning, J.I. (2006). Temporal coding mediates discrimination of “bitter” taste stimuli by an insect. Journal of Neuroscience *26*, 8900–8908.
9. Scott, K., Brady, R., Cravchik, A., Morozov, P., Rzhetsky, A., Zuker, C., and Axel, R. (2001). A chemosensory gene family encoding candidate gustatory and olfactory receptors in *Drosophila*. Cell *104*, 661–673.
10. Dahanukar, A., Lei, Y.T., Kwon, J.Y., and Carlson, J.R. (2007). Two Gr genes underlie sugar reception in *Drosophila*. Neuron *56*, 503–516.
11. Whitehead, A.T., and Larsen, J.R. (1976). Electrophysiological responses of galeal contact chemoreceptors of *Apis mellifera* to selected sugars and electrolytes. Journal of Insect Physiology *22*, 1609–1616.
12. Glendinning, J.I., and Hills, T.T. (1997). Electrophysiological evidence for two transduction pathways within a bitter-sensitive taste receptor. Journal of Neurophysiology *78*, 734–45.
13. Hiroi, M., Marion-Poll, F., and Tanimura, T. (2002). Differentiated response to sugars among labellar chemosensilla in *Drosophila*. Zoological Science *19*, 1009–1018.

14. Kessler, S., Vlimant, M., and Guerin, P.M. (2013). The sugar meal of the African malaria mosquito *Anopheles gambiae* and how deterrent compounds interfere with it: a behavioural and neurophysiological study. The Journal of Experimental Biology *216*, 1292–306.

15. Martelli, C., Carlson, J.R., and Emonet, T. (2013). Intensity invariant dynamics and odor-specific latencies in olfactory receptor neuron response. Journal of Neuroscience *33*, 6285–6297.

16. Inoue, T.A., Asaoka, K., Seta, K., Imaeda, D., and Ozaki, M. (2009). Sugar receptor response of the food-canal taste sensilla in a nectar-feeding swallowtail butterfly, *Papilio xuthus*. Naturwissenschaften *96*, 355–363.

17. Reiter, S., Campillo Rodriguez, C., Sun, K., and Stopfer, M. (2015). Spatiotemporal coding of individual chemicals by the gustatory system. Journal of Neuroscience *35*, 12309–12321.

18. Chapman, R.F., Ascoli-Christensen, A., and White, P.R. (1991). Sensory coding for feeding deterrence in the grasshopper *Schistocerca americana*. Journal of Experimental Biology *158*, 241–259.

19. Nicolson, S.W., Nepi, M., and Pacini, E. (2007). Nectaries and Nectar. pp. 215-264 (Berlin: Springer)

20. Krenn, H.W., Plant, J.D., and Szucsich, N.U. (2005). Mouthparts of flower-visiting insects. Arthropod Structure and Development *34*, 1–40.

21. Pouzat, C., Mazor, O., and Laurent, G. (2002). Using noise signature to optimize spike-sorting and to assess neuronal classification quality. Journal of Neuroscience Methods *122*, 43–57.

22. Hill, D.N., Mehta, S.B., and Kleinfeld, D. (2011). Quality metrics to accompany spike sorting of extracellular signals. The Journal of Neuroscience *31*, 8699–8705.

23. Su, C.-Y., Menuz, K., Reisert, J., and Carlson, J.R. (2012). Non-synaptic inhibition between grouped neurons in an olfactory circuit. Nature *492*, 66–71.

24. Weiss, S. a, Preuss, T., and Faber, D.S. (2008). A role of electrical inhibition in sensorimotor integration. Proceedings of the National Academy of Sciences of the United States of America *105*, 18047–52.

25. Blot, A., and Barbour, B. (2014). Ultra-rapid axon-axon ephaptic inhibition of cerebellar Purkinje cells by the pinceau. Nature Neuroscience *17*, 289–95.

26. Galarreta, M., and Hestrin, S. (2001). Electrical synapses between GABA-releasing interneurons. Nature Reviews Neuroscience *2*, 425–433.

27. Blatow, M., Rozov, A., Katona, I., Hormuzdi, S.G., Meyer, A.H., Whittington, M.A., Caputi, A., and Monyer, H. (2003). A novel network of multipolar bursting

interneurons generates theta frequency oscillations in neocortex. Neuron *38*, 805–817.

28. Spong, K.E., and Robertson, R.M. (2013). Pharmacological blockade of gap junctions induces repetitive surging of extracellular potassium within the locust CNS. Journal of Insect Physiology *59*, 1031–1040.

29. Calkins, T.L., and Piermarini, P.M. (2015). Pharmacological and genetic evidence for gap junctions as potential new insecticide targets in the yellow fever mosquito, *Aedes aegypti*. PLoS ONE *10*, 1–15.

30. Wright, G.A., Mustard, J.A., Simcock, N.K., Ross-Taylor, A.A.R., McNicholas, L.D., Popescu, A., and Marion-Poll, F. (2010). Parallel reinforcement pathways for conditioned food aversions in the honeybee. Current Biology *20*, 2234–2240.

31. Charlu, S., Wisotsky, Z., Medina, A., and Dahanukar, A. (2013). Acid sensing by sweet and bitter taste neurons in *Drosophila melanogaster*. Nature Communications *18*, 1199–1216.

32. Gothilf, S., Galun, R., and Bar-Zeev, M. (1971). Taste reception in the Mediterranean fruit fly: Electrophysiological and behavioural studies. Journal of Insect Physiology *17*, 1371–1384.

33. Cocco, N., and Glendinning, J.I. (2012). Not all sugars are created equal: some mask aversive tastes better than others in an herbivorous insect. Journal of Experimental Biology *215*, 1412–1421.

34. Ozaki, M., and Amakawa, T. (1992). Adaptation-promoting effect of IP3, Ca2+, and phorbol ester on the sugar taste receptor cell of the blowfly, *Phormia regina*. Journal of General Physiology *100*, 867–879.

35. Kwon, H., Ali Agha, M., Smith, R.C., Nachman, R.J., Marion-Poll, F., and Pietrantonio, P. V. (2016). Leucokinin mimetic elicits aversive behavior in mosquito *Aedes aegypti* and inhibits the sugar taste neuron. Proceedings of the National Academy of Sciences *113*, 6680–6685.

36. Ma, C., Kessler, S., Simpson, A., and Wright, G. (2016). A novel behavioral assay to investigate gustatory responses of individual, freely-moving bumble bees (*Bombus terrestris*). Journal of Visualized Experiments, 1–7.

37. Golding, N.L., Jung, H.Y., Mickus, T., and Spruston, N. (1999). Dendritic calcium spike initiation and repolarization are controlled by distinct potassium channel subtypes in CA1 pyramidal neurons. The Journal of Neuroscience *19*, 8789–98.

38. Lemon, N., and Turner, R.W. (2000). Conditional spike backpropagation generates burst discharge in a sensory neuron. Journal of Neurophysiology *84*, 1519–1530.

39. Larkum, M.E., Zhu, J.J., and Sakmann, B. (1999). A new cellular mechanism for coupling inputs arriving at different cortical layers. Nature *398*, 338–341.

40. Krahe, R., and Gabbiani, F. (2004). Burst firing in sensory systems. Nature Reviews Neuroscience *5*, 13–23.

41. Pereda, A.E. (2014). Electrical synapses and their functional interactions with chemical synapses. Nature Reviews Neuroscience *15*, 250–263.

42. Jaslove, S.W., and Brink, P.R. (1986). The mechanism of rectification at the electrotonic motor giant synapse of the crayfish. Nature *323*, 63–65.

43. Phelan, P., Goulding, L.A., Tam, J.L.Y., Allen, M.J., Dawber, R.J., Davies, J.A., and Bacon, J.P. (2008). Molecular mechanism of rectification at identified electrical synapses in the *Drosophila* giant fiber system. Current Biology *18*, 1955–1960.

44. Gordon, M.D., and Scott, K. (2009). Motor control in a *Drosophila* taste circuit. Neuron *61*, 373–384.

45. Clark, M.G., Bloxham, D.P., Holland, P.C., and Lardy, H.A. (1973). Estimation of the fructose diphosphatase-phosphofructokinase substrate cycle in the flight muscle of *Bombus affinis*. The Biochemical Journal *134*, 589–97.

46. Stabler, D., Paoli, P.P., Nicolson, S.W., and Wright, G.A. (2015). Nutrient balancing of the adult worker bumblebee (*Bombus terrestri*s) depends on the dietary source of essential amino acids. Journal of Experimental Biology *218*, 793–802.

47. Getting, P.A. (1971). The sensory control of motor output in fly proboscis extension. Zeitschrift für Vergleichende Physiologie *74*, 103–120.

48. Itskov, P.M., Moreira, J.-M., Vinnik, E., Lopes, G., Safarik, S., Dickinson, M.H., and Ribeiro, C. (2014). Automated monitoring and quantitative analysis of feeding behaviour in *Drosophila*. Nature Communications *5*, 4560.

49. Robertson, H.M., and Wanner, K.W. (2006). The chemoreceptor superfamily in the honey bee, *Apis mellifera*: Expansion of the odorant, but not gustatory, receptor family. Genome Research *16*, 1395–1403.

50. Bitterman, M.E., Menzel, R., Fietz, A., and Schäfer, S. (1983). Classical conditioning of proboscis extension in honeybees (*Apis mellifera*). Journal of Comparative Psychology *97*, 107–119.

51. Hodgson, E.S. (1958). Electrophysiological studies of arthropod chemoreception. III. Chemoreceptors of terrestrial and fresh-water arthropods. The Biological Bulletin *115*, 114–125.

52. Kuwabara, M. (1957). Bildung des bedingten Reflexes von Pavlovs Typus bei der Honigbiene, *Apis mellifica*. Hokkaido University Collection of Scholarly Academic Papers *13*, 458–464.

53. Aldworth, Z.N., and Stopfer, M.A. (2015). Trade-off between information format and capacity in the olfactory system. The Journal of neuroscience *35*, 1521–9.

54. Ritz, C., Baty, F., Streibig, J.C., and Gerhard, D. (2015). Dose-response analysis using R. PLoS ONE *10*, 1–13.

Figures legends

Figure 1. Two GRNs in an A-type sensillum exhibit coherent, burst spiking when stimulated with 100 mM sucrose. (A) Scanning electron micrograph of the galea, labial palps and glossa of the bee proboscis. (B) The galea possess the longer 'A-type' sensilla (~20 µm, red arrows) and the shorter 'B-type' sensilla (~10 µm, black arrows), and each has a diameter of ~4 µm. (C) Transmission electron micrograph of a cross section at the base of an 'A-type' sensillum shows that it houses the dendrites [d] of 4 GRNs. These dendrites are ~0.25 µm in diameter, and are tightly clustered within an inner lymphatic cavity [i] which is encompassed by an outer lymphatic cavity [o]. The figure shows two overlaid images; the dotted box indicates a higher resolution image. (D) Simultaneous recordings made using 'tip' (top; black trace) and 'tungsten' (bottom; blue trace) electrodes from an A-type sensillum before and after stimulus onset. Open circles indicate spike positions. (E) **Top**: A segment of the bandpass filtered (300-3000 Hz; black trace, tip recording; blue trace, tungsten recording) recording used for spike sorting. **Bottom**: Spike sorting revealed two distinct waveforms on both channels, termed as GRN 1 (grey) and GRN 2 (magenta) spikes. (F) Example superposition waveforms that arise when a GRN 1 and a GRN 2 spike fire within 2 ms of each other. Each row represents a different temporal separation between spikes. Open circles indicate spike positions. The grey trace represents a recording with 3 ms between the spikes of each GRN. (G) **Left:** A rose plot derived from a Hilbert's transform on 10-100 Hz filtered tungsten traces using 1 s of recording. **Right:** A sample unfiltered tungsten recording trace shows the typically observed coherent spike timing of both GRNs; GRN 1 fires within bursts around the peak of the oscillation and GRN 2 fires a single spike at the end of bursts near the falling phase of the oscillation. Data for E-G l were obtained from the recording shown in D. See also Figure S1.

Figure 2. Spikes from each sensillum are transmitted via the maxillary nerve (MxN) (A) Recording setup for monitoring MxN nerve activity using a tungsten wire electrode during stimulation of an A-type sensillum with a tip electrode. (B) Both channels of recording reveal bursts of spikes (open circles), low frequency oscillations, superposition features (bars) and

distinct shorter spike shapes (GRN 2 spikes) at end of burst positions (closed circles). (C) Simultaneous recordings from two neighboring A-type sensilla (sensillum 1 (S1), top; sensillum 2 (S2), middle) and the MxN (bottom trace). The MxN recording shows spikes (dots) and oscillations summed across both sensilla. (D) (top panel) A spike time cross-correlogram between the spike times from S1 and S2 shows that the spiking in each sensillum is not correlated (black trace). The cross-correlation between the cumulative spike times across both sensilla (S1+S2) and the MxN (blue trace). (bottom panel) A cross-correlogram between the 10-60 Hz filtered recordings from S1 and S2 shows an absence of correlation in low frequency components (black trace). Adding these low frequencies from both sensilla (S1+S2) however does show coherence with the MxN (blue trace), indicating that the MxN carries the oscillatory components of both sensilla. Cross-correlograms in both panels are averages over 3 trials from the same sensillum.

Figure 3. Bursting GRNs exhibit specific spike timing and different rates of adaptation. (A) Tip recording from an A-type sensillum stimulated with 100 mM sucrose (black trace). Linear regressions (dashed lines) were fit to the ISIs of GRN 1 (closed grey circles) and GRN 2 (closed magenta circles) over the first 2 s. (B) Spikes from GRN 1 (open grey circles) and GRN 2 (open magenta circles) in a sample burst. The rate of change in the GRN 1 ISIs (i.e. GRN 1 slope; closed black circles) is represented by the linear fit (red line). (C) The magnitude of the slope of the within-burst linear fits was plotted as a function of the total burst duration; these data were modeled as an exponential equation ($a*exp^{b*x}$). When the GRN 2 ISI is <0.06 s, the slope of GRN 1 ISI within bursts is negative, indicating that GRN1 spiking accelerates. N=453 bursts, 34 recordings, 1-2 recordings per bee, using recordings with at least 3 bursts. (D) Averages of the linear regressions made to 2 s recordings for the GRN 1 ISIs (grey; 0.003 $\pm$ 0.002 s / 2 s, mean $\pm$ SD, n=21 recordings, 1-2 sensilla per animal) and the GRN 2 ISIs (magenta; 0.033 + 0.021 s / 2 s). On average, GRN 2 slows to an ISI of 0.06 s within 1 s from stimulus onset (dashed lines). Shaded region represents 1*SD at each time point. (E) Example tip recording showing segments of a 30 s stimulation with 100 mM sucrose. After spike sorting (see methods), the GRN 2 spike waveform with its relatively larger after-hyperpolarization is clearly seen later in the recording (bottom trace; magenta circles). This suggests that the oscillations in voltage associated with bursting are due to the after-hyperpolarization that follows each GRN 2 spike. (F) Cross correlation of GRN 2 spike times with GRN 1 (average correlation shown by black trace, individual recordings shown by grey traces, n=5 animals, 1 recording per animal, 30 s

stimulations with 100 mM sucrose). The sharp drop in correlation after 0 s reflects the silence in spiking activity following GRN 2 spikes. GRN 1 activity recovers ~0.025 s after the GRN 2 spikes (time taken for the correlation to reach half of the baseline value). The dip in correlation around -0.002 ms is indicative that GRN 2 spiking activity is weakly dependent on the time following a GRN 1 spike. (G) GRN 1 spiking fails to adapt or adapts slowly when GRN 2 exhibits strong firing (>10 GRN 2 spikes in the first 1 s; magenta lines, mean shown as dashed line, N=11 recordings, 11 animals); GRN1 adapts relatively rapidly when GRN 2 spikes infrequently (<10 GRN 2 spikes in first 1 s; grey lines, N = 4). See also Figure S2.

Figure 4. Bursting allows GRN 1 to resist spike frequency adaptation. (A) Example recordings from 10 mM CBX application protocol. **Top**: Initial stimulation with 100 mM sucrose (Initial). **Middle:** After immersing the tip of the sensillum in 10 mM Cbx for 2 min, bursting is suppressed during stimulation with 100 mM sucrose (Post-$CBX_{10\ mM}$). **Bottom:** The burst response is recovered during stimulation with 100 mM sucrose after allowing at least a 5 min period after CBX exposure (Recovery). All three recordings were made from the same sensillum. (B) Mean GRN 2 spiking activity (crosses) during the 1 s stimulation with 100 mM sucrose is significantly reduced after CBX exposure (1-way ANOVA on log(GRN 2 spike count + 1), $F_{2,17}$=69.8, *** p<0.001). (C) Spike sorting recordings shown in (A; see methods) reveals that CBX exposure inhibits GRN 2 activity. Plotting the first two principal components (PC; B left column) reveal two active GRNs (GRN 1, grey; GRN 2, magenta) for the initial sucrose stimulation (top) and recovery (bottom), but not after 10 mM CBX exposure (middle). Spikes in the time period between 1 – 4 s after stimulus onset were used for sorting. Corresponding spike waveforms are shown in the right column. Amplitude of waveforms are relative to the median absolute deviation (MAD) of the channel data (channel data was normalized to the MAD). (D) Average of 3-parameter logarithmic fits made to GRN 1 ISIs over a 5 s stimulation period for each stimulation protocol shown in (A). Shaded region represents 1*SD at each time point. N=6 animals, 1 recording/animal. See also Figure S3 and Table S1.

Figure 5. Bumblebee bursting GRNs maintain the highest rate of spiking during prolonged stimulation. (A) Tip recordings from galeal sensilla from 4 different bee species reveal that burst spiking involving GRN 1 (open circles) and GRN 2 (solid circles) is common to bee species. (B) Data from 8 insect species reported from the literature (see main text)

were compared to 5 s tip recordings from bumblebees. The slope of each line is reported for each species (measured at the indicated time points with respect to the ISI at 0 s). The bumblebees' (*B. terrestris* and *Bombus pascuorum)* GRN 1 had the lowest rate of adaptation over the 5 s interval. For the *Bombus sp.* and *A. mellifera*, spike rate was calculated from 3-term logarithmic fits made to ISI data (see Figure S1 G) and averaged over recordings. *B. pascuorum*: N = 1-2 sensilla from 4 bees; *B. terrestris*: N = 1-2 sensilla from 15 bees; *A. mellifera* N=1-2 sensilla from 5 bees.

Figure 6. Rate of bursting is concentration dependent and is correlated to feeding behavior (A) Tip recordings obtained from an A-type sensillum with different concentrations of sucrose show that the spiking and burst response depend on concentration. (B) Tungsten recordings from an A-type sensillum show that stimulation with 100 mM of sucrose and fructose evoke the burst response. Few bursts are evoked by 100 mM glucose. (C-D) Tip recordings reveal that (C) the rate of GRN 1 spiking (measured as spiking frequency) and (D) the rate of GRN 2 spiking (i.e., burst frequency) increased as a log-logistic function of sucrose, fructose and glucose concentration. The EC_{50}, or the point at which the rate of firing reaches half of its maximum value, is indicated by the 'x' in each plot. N $\geq$10 bees/sugar. (E) The probability of producing the proboscis extension reflex (PER) depended on stimulus concentration and sugar identity. **Top:** Time to PER was 0.8 ± 0.6 s from stimulus onset (median ± IQR; dashed black line; data pooled across all three sugars and across all concentrations). **Bottom:** PER was evoked for fructose at concentrations >250 mM, and for both sucrose and glucose at concentrations >500 mM. N=8/conc/sugar. (F) The amount of food consumed (during the first 10 min of the feeding period) was plotted against the time the proboscis was in contact with the food (during the first 2 min of the feeding period). The average value for the responses of bees to each of the sugars at each concentration (0, 1, 10, 50, 100, 1000 mM from left to right) was plotted. Sample size: 7 $\leq$ N $\leq$ 13/conc/sugar. See also Figure S4.

STAR★Methods

1. Experimental Model and Subject Details

Bees

Experiments were performed on female (worker) *Bombus terrestris audax* (Koppert Biological Systems, NATURPOL, Netherlands), collected as they tried to exit the colony. Colonies were

maintained at 24 ±1°C and 28 ±1% relative humidity with natural light conditions, and fed commercial pollen and sugar solution bee food. *Bombus pascuorum* have been provided by Hauke Koch and Phil Stevenson from their rearing established at Kew Botanical Garden, UK. *Bombus hortorum* and *Bombus lapidarius* were caught while foraging on flowers around Newcastle University in Newcastle upon Tyne, U.K. Honeybees (*Apis mellifera* var. Buckfast) were obtained from free-flying outdoor colonies originally obtained from the U.K National Bee Unit (Sand Hutton, Yorkshire).

2. Method Details

Transmission Electron Microscopy (TEM)

TEM was done at the Electron Microscope Research Services, Newcastle University. The distal 1 mm of adult female worker galea were ablated and fixed in 2% glutaraldehyde in 0.1 M cacodylate buffer overnight at 4º C. Samples were then washed with cacodylate buffer (3 x 15 min washes) and left in the buffer overnight at 4º C. Samples were then fixed in 1% osmium tetroxide in deionised water for 1 hour. After washing with deionised water (2 x 15 min washes), samples were dehydrated in increasing concentrations of acetone in deionised water (25% acetone for 30 min, 50% for 30 min, 75% for 30 min, 2 x 100% for 1 hour). A TAAB epoxy medium resin kit (TAAB Lab Equiptment, UK) was used to impregnate the samples with increasing concentration of resin in acetone (25% resin for 1 hour, 50% for 1 h, 75% for 1 h, 100% for 1h). After leaving overnight in a rotator, the samples were impregnated again with resin (2 x 100% resin for 1h, 1 x 100% resin for 3 h). Samples were then embedded in capsules in 100 % resin and placed in 60º C oven for 24-36 h.

Embedded samples were then sectioned using a diamond knife on an ultramicrotome (Leica EM UC7, Leica UK Ltd). 70 nm sections were stretched with chloroform to eliminate compression and mounted on Pioloform-filmed copper grids. Grids were stained using 2% aqueous uranyl acetate-lead citrate (supplied by Leica). Grids were examined using a Philips CM 100 Compustage (FEI) Transmission Electron Microscope and digital images collected using an AMT CCD camera (Deben, UK).

Electrophysiological recordings

To obtain recordings from galeal sensilla, bees were first chill-immobilized and harnessed as described in [50]. To prevent movement, mouthpart nerves were then severed by making an incision at the base of the mouthparts. The galea were then oriented with the help of wire pins on a wax base. Two recording methods were used to monitor the activity of GRNs at the level of the sensillum: 1) The tip electrode technique [51] where a capillary electrode filled with tastant solution in demineralized water (no electrolyte used) placed at the tip of the sensillum, and 2) a sharpened tungsten electrode inserted punctured ~1 mm into the base of the sensillum. Electrodes were positioned using a motorized micro-manipulator (MPC-200, Sutter Instrument, USA). A minimum latency period of 3 minutes was allowed between stimulations from the same sensillum to avoid

adaptation. To measure responses from the maxillary nerve, a 25 µm OD tungsten wire was used, with ~0.5 mm of the polyamide insulation removed from the tip. The wire was pushed into the base of an ablated galea, until it reached a position ~2 mm from the tip of the galea (near the maxillary palp), and was positioned close to the maxillary nerve. This wire was connected to a headstage (AM-systems 1800, USA). Sensilla were stimulated using the tip recording technique. The tip electrode was connected to a TastePROBE amplifier (SYNTECH, Germany; Marion-Poll & van der Pers, 1996), which was in turn connected to an AM-systems 1800 amplifier. Signals from the recording electrodes were pre-acquisition filtered between 10 Hz-10 kHz and a gain of 100x was applied. Signals were then digitized (DT9803 Data Translation) and acquired using DbWave (version 4.2014.3.22). Acquired signals were imported into MATLAB R2016a (The Mathworks) for analysis. Using MATLAB, stimulus onset and offset were determined by the contact artifacts from the tip electrode recording. Signals were filtered in the appropriate pass-band using a 2nd order Butterworth filter. Band-stop filters constructed using a 1 Hz window around 50, 100, 150 and 200 Hz were used to remove line noise frequencies. Filtered signals were then normalized to their noise estimates, calculated as 1.48 times the median absolute deviation (MAD) of the filtered signal. The MAD is a measure similar to the standard deviation (SD), but is not sensitive to the presence of outliers in the dataset. 1.48 is a constant that is used when the distribution is normal, as is the case for the distribution of noise frequencies.

Pharmacology

Sensilla were initially stimulated with 100 mM sucrose using the tip electrode recording method. Following this, a capillary electrode filled with either water, carbenoxolone disodium salt (1 mM, 5 mM or 10 mM) or NaCl (20 mM) was placed on the tip of the sensillum for 2 minutes. A minimum of a 5 minute period was allowed for the GRNs to recover before stimulating again with 100 mM sucrose.

Behavior

Two assays were used to study bee feeding behavior in response to stimulation with sugars. In the first assay, a modified version of the proboscis extension reflex assay (PER, Kuwabara, 1957) was used to examine the initiation of feeding. To measure behavioural responses in function of sugar concentrations, bumblebees were harnessed and starved for 3 to 8 h at room temperature in a dark environment. Mouthparts were stimulated with a droplet of tastant stimuli of varying concentrations. Behaviors were video recorded with a digital microscope (Dino-Lite AM4815ZT, UK), and a custom-made MATLAB program was used to track the position of the mouthparts. This was done by defining a movement threshold as two times the maximum movement obtained from the water stimulus. To test whether the probability of eliciting movement of the proboscis or the PER behaviors depends on concentration and sugars, separate logistic regressions were fitted to the data for each behavior. In

the second assay, the feeding behaviour during the first feeding bout was assessed using a protocol for individual, freely-moving bumblebees (for a detailed protocol see [36]). Briefly, individual bees were collected from commercially-reared colonies and starved for ~4 h in a plastic holding vial. Each bee was transferred to a testing arena (a modified 15 ml centrifuge tube). The testing arena had a digitial microscope camera positioned at the end where testing was performed. Bees were baited using a 1 M sucrose solution to teach them to extend their proboscis. The test solution was applied in a microcapillary tube within 30 s of the bait solution and the behaviour of the bee was recorded for 2 min. The volume of solution consumed in the 2 min period was recorded by scanning the microcapillary tube before and after the test. The following behaviours were scored from the video offline: proboscis extended, contact with solution, or bee out of frame of video (as in [36]). Data for the number of contacts, duration of the first feeding bout, and the total time in contact with the solution were analyzed from the videos using generalized linear modeling in SPSS.

3. Quantification and Statistical Analysis

The number of bees (N) along with the number of sensilla used per bee for the various analyses are mentioned either in the main text or in the figure legends. Data are judged to be statistically significant when $p < 0.05$ in applied statistical analysis. One-way analysis of variance (ANOVA) and linear regression were only used if the variance between groups was not significant (i.e., $p > 0.05$ using Bartlett's test for equal variances and $p > 0.05$ using Shapiro-Wilks test for normality). If a 1-way ANOVA indicates that the groups have different means, then the MATLAB function multcompare was used to do post-hoc multiple comparisons. All models (ANOVA, linear regression, GLMs and least square differences) were fitted with either MATLAB, R or SPSS and were checked for the appropriate distribution of residuals.

Spike Sorting

Spike waveforms obtained from both the tip and tungsten electrodes were sorted using a semi-automated, model-based spike sorting method [21;22] that has been used for spike sorting of gustatory recordings in *M.sexta* [17], implemented in MATLAB by the lab of Dr. Mark Stopfer (e.g. see [53]). This method can be divided into two steps: clustering and classification. In the clustering step, spike waveforms are first detected from a 0.1-1.1 s window after stimulus onset. A series of thresholds are then used to 1) choose a window around the peak of the spike waveform to use for comparisons, 2) remove a segment around the peak of each action potential, and 3) remove superposition waveforms that lie outside a threshold standard deviation envelope around the waveforms. Noisy waveforms can arise due to artifacts in the recording, or from superposition features that arise when multiple neurons fire action potentials very close together such that their waveforms add together.

A principal component analysis (PCA) is then done on the segments of the spike waveforms that remain after these three steps of thresholding. The first 5 principal components are then used to divide the dataset into two clusters, since there was evidence of at least two separate GRNs active in the 100 mM sucrose recordings. The quality of clustering was estimated by 1) plotting the residuals of each cluster (average of differences between each spike waveform from the median waveform of the cluster). Recordings are only used if the residuals fall near a 95% confidence interval set around the noise estimate for the trace. 2) A Fisher's Linear Discriminant Analysis (LDA) between the two clusters using the 5 principal components obtained from the PCA. The Fisher's LDA projects data onto the axis that is best for separation of different clusters. If clusters are not well separated, the LDA reports a small 'distance' value between the two clusters. Recordings are used only if the Fisher's LDA yields a distance > 4. The median spike waveform of each cluster was used as the cluster template.

In the classification stage, each spike waveform in the recording is attributed to a cluster. First, superposition waveforms are detected. This is done by setting a Mahalanobis distance threshold; any waveform having a distance greater than this threshold is considered a superposition spike. Superposition spikes are then classified to superposition templates, while the remaining spikes are classified to the cluster templates, using a minimum Euclidean distance measure. To estimate the quality of classification, the percentage of Type-1 and Type-2 errors are obtained, which result from 1) false positives from refractory period violations, 2) false positives and false negatives due to overlap between both clusters, and 3) false negatives due to missed spikes from thresholding during detection. If the cumulative errors fell under 10% of the dataset, the recording was considered well classified and was used for analysis. The same procedure was followed for sorting spikes obtained from the single channel tip recordings. For 30 s recordings, only spikes in the 1-30 s duration from stimulus onset were used for sorting, and for 5 s recordings the spikes in the 1-3 s duration were used.

Frequency analysis

To measure the frequency of oscillations, recordings were first bandpass filtered between 10-3000 Hz. Then, Welch's averaged periodogram method was used to estimate the Power Spectral Density (PSD) of the recording trace, using a Hanning window of 6000 samples and a 300 sample overlap, for 0.1 Hz increments between 10-100 Hz. For tungsten recordings, the PSD was estimated for three time windows: 0.7 to 0.2 s before stimulus onset, 0.1 to 0.6 s after stimulus onset and 0.2 to 0.7 s after stimulus offset. The values presented in the figures are powers scaled by the equivalent noise bandwidth of the window.

Burst detection

End of burst positions (i.e., spiking events that were positioned at the end of each burst) were

detected from the inter-spike intervals (ISIs) of a recording. The ISI for each spike event was calculated as the duration following the spike until the subsequent spike event. ISIs less than 0.002 s were first removed. A logarithmic curve having equation *y(x)=a*log(b*x+c)* was fit to the spike timestamps (i.e., the position, in seconds, of each spike event; *x*) vs ISI (*y*). The lower and upper limits of *a*,*b* and *c* were set as 0 and infinity, respectively. Weights proportional to *1/y* (inverse of ISI) were used, and the fit was made using robust least-squares regression. A spike was considered as an end of burst spike if its ISI exceeded a value of 2 times the fit at that time point. ISIs were only detected from traces having a minimum of 4 spikes, otherwise the trace was considered to have no bursts. See Figure S1 G for example.

Spike and burst frequencies in function of concentration

To evaluate the effect of the sugar concentrations on the spiking and bursting rates generated by the GRNs, a 3-parameters log-logistic model of the form :

$$f(x) = \frac{b}{1+e^{a(log(x)-log(c))}}$$

was fitted to the data with the drm command from the R (3.3.3) package drc [54]. *x* denotes the dose (i.e., concentration), *f(x)* denotes the response (i.e spike frequency), a denotes the steepness of the dose-response curve, *b* denotes the upper asymptote or the maximum response, and *c* denotes the EC_{50} (i.e., the concentration where 50% of the maximum response is reached). The effect of the sugar treatments was assessed by testing the change in deviance (using F-tests) between the minimal model (where all the sugars where grouped in one factor level) and the maximal model (where each sugar was considered as a separate factor level). F-tests between these two nested models were computed using the ANOVA command [54]. Significant differences between the sugar models for the *c* parameter (EC_{50}) and the *b* parameter (upper asymptote) were assessed using the compParm command.

Further information and requests for data should be directed to the Lead Contact, Geraldine Wright (jeri.wright@ncl.ac.uk).

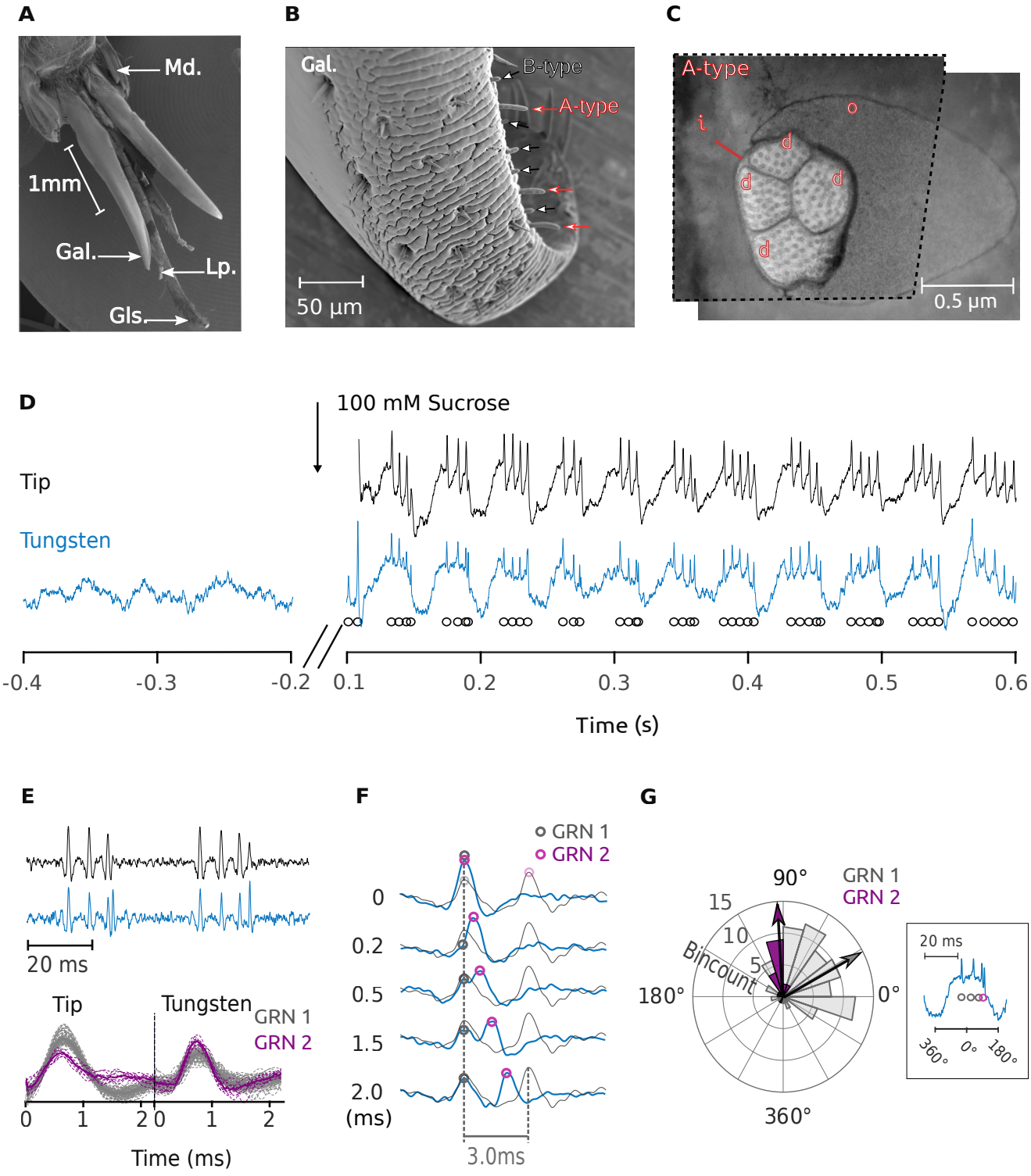
A
Md.
1mm
Gal.
Lp.
Gls.
B
Gal.
B-type
A-type
50 µm
C
A-type
i
o
d
d
d
d
0.5 µm
D
100 mM Sucrose
Tip
Tungsten
-0.4
-0.3
-0.2
0.1
0.2
0.3
0.4
0.5
0.6
Time (s)
E
20 ms
Tip
Tungsten
GRN 1
GRN 2
0
1
2
0
1
2
Time (ms)
F
GRN 1
GRN 2
0
0.2
0.5
1.5
2.0
(ms)
3.0ms
G
90°
GRN 1
GRN 2
15
10
5
Bincount
180°
0°
360°
20 ms
360°
0°
180°

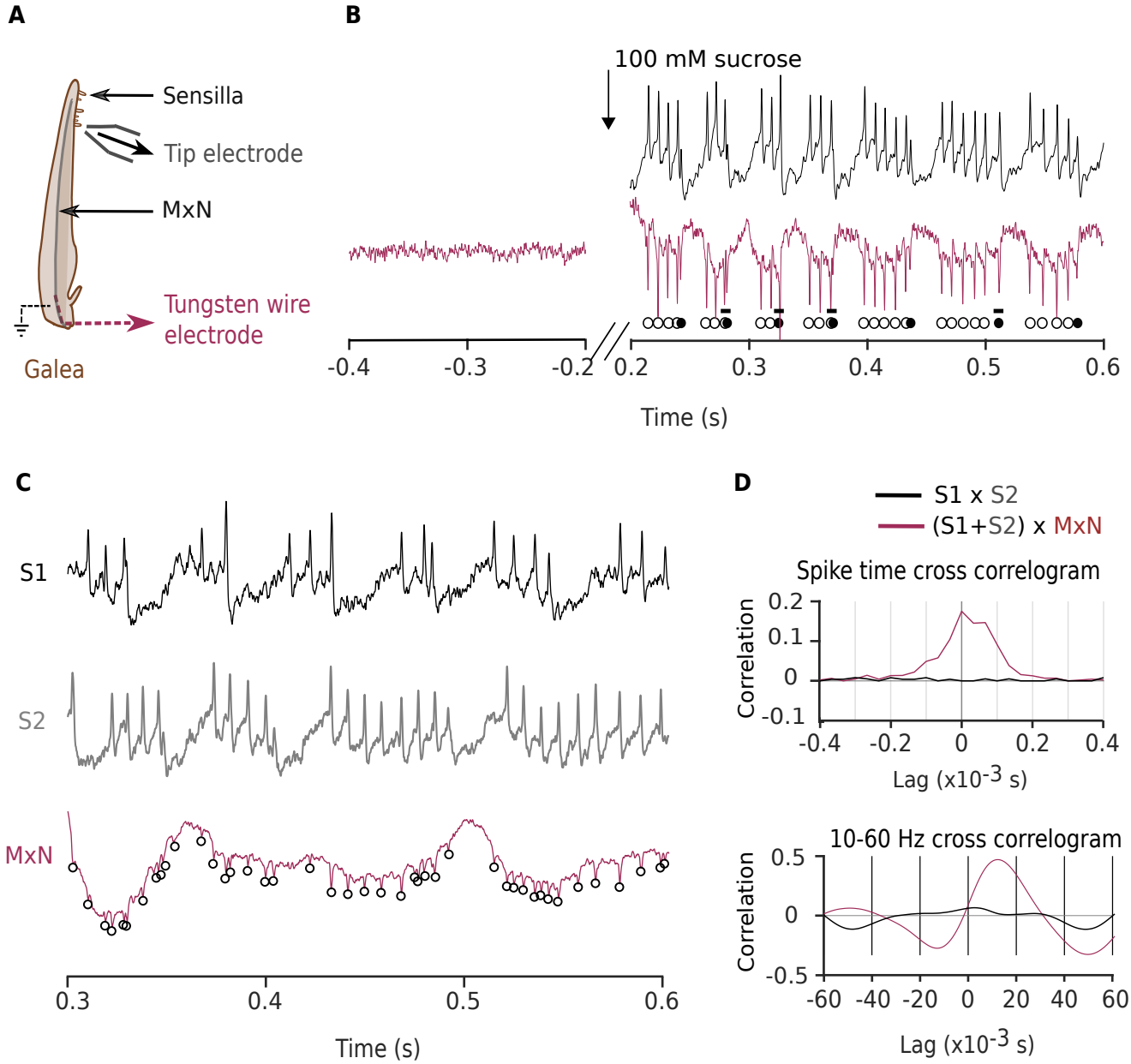
A
Sensilla
Tip electrode
MxN
Tungsten wire electrode
Galea
B
100 mM sucrose
-0.4
-0.3
-0.2
0.2
0.3
0.4
0.5
0.6
Time (s)
C
S1
S2
MxN
0.3
0.4
0.5
0.6
Time (s)
D
S1 x S2
(S1+S2) x MxN
Spike time cross correlogram
Correlation
0.2
0.1
0
-0.1
-0.4
-0.2
0
0.2
0.4
Lag (x10-3 s)
10-60 Hz cross correlogram
Correlation
0.5
0
-0.5
-60
-40
-20
0
20
40
60
Lag (x10-3 s)

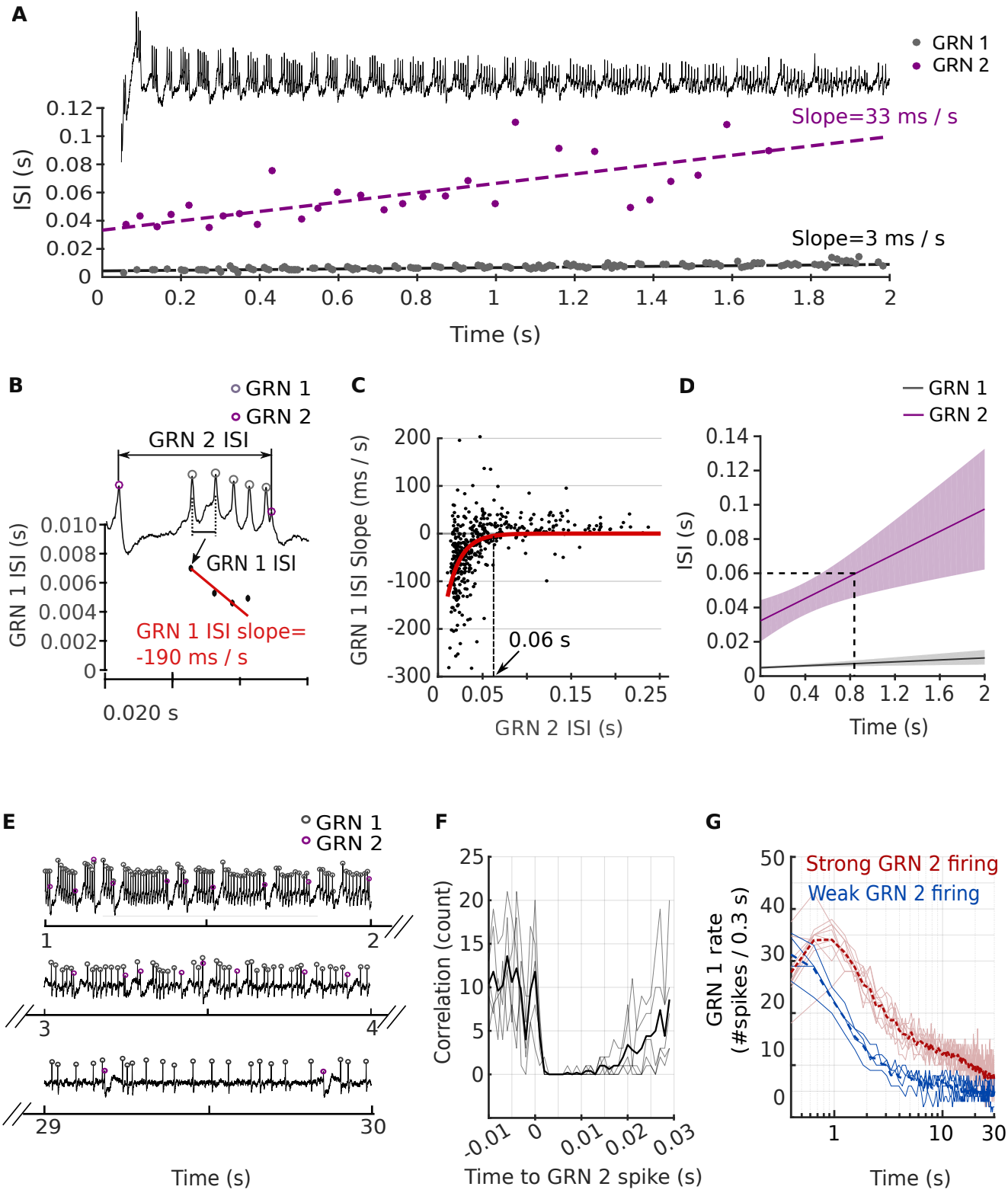
A
GRN 1
GRN 2
Slope=33 ms / s
Slope=3 ms / s
ISI (s)
Time (s)
B
GRN 1
GRN 2
GRN 2 ISI
GRN 1 ISI
GRN 1 ISI slope=
-190 ms / s
GRN 1 ISI (s)
0.020 s
C
GRN 1 ISI Slope (ms / s)
0.06 s
GRN 2 ISI (s)
D
GRN 1
GRN 2
ISI (s)
Time (s)
E
GRN 1
GRN 2
Time (s)
F
Correlation (count)
Time to GRN 2 spike (s)
G
Strong GRN 2 firing
Weak GRN 2 firing
GRN 1 rate
(#spikes / 0.3 s)
Time (s)

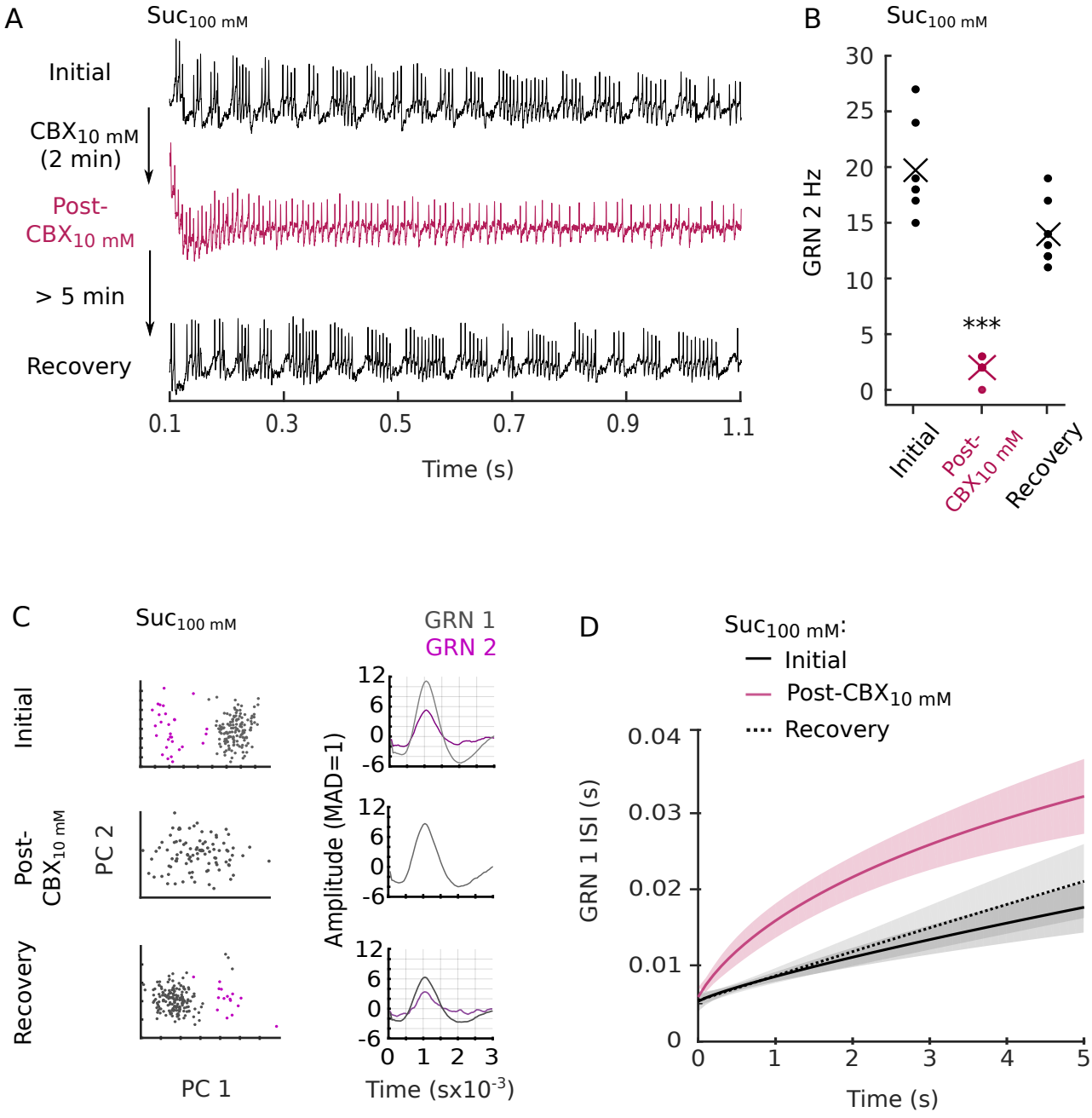
A
Suc100 mM
Initial
CBX10 mM
(2 min)
Post-
CBX10 mM
> 5 min
Recovery
0.1
0.3
0.5
0.7
0.9
1.1
Time (s)
B
Suc100 mM
GRN 2 Hz
30
25
20
15
10
5
0
***
Initial
Post-
CBX10 mM
Recovery
C
Suc100 mM
GRN 1
GRN 2
Initial
Post-
CBX10 mM
Recovery
PC 2
PC 1
Amplitude (MAD=1)
12
6
0
-6
0 1 2 3
Time (sx10-3)
D
Suc100 mM:
Initial
Post-CBX10 mM
Recovery
GRN 1 ISI (s)
0.04
0.03
0.02
0.01
0
0 1 2 3 4 5
Time (s)

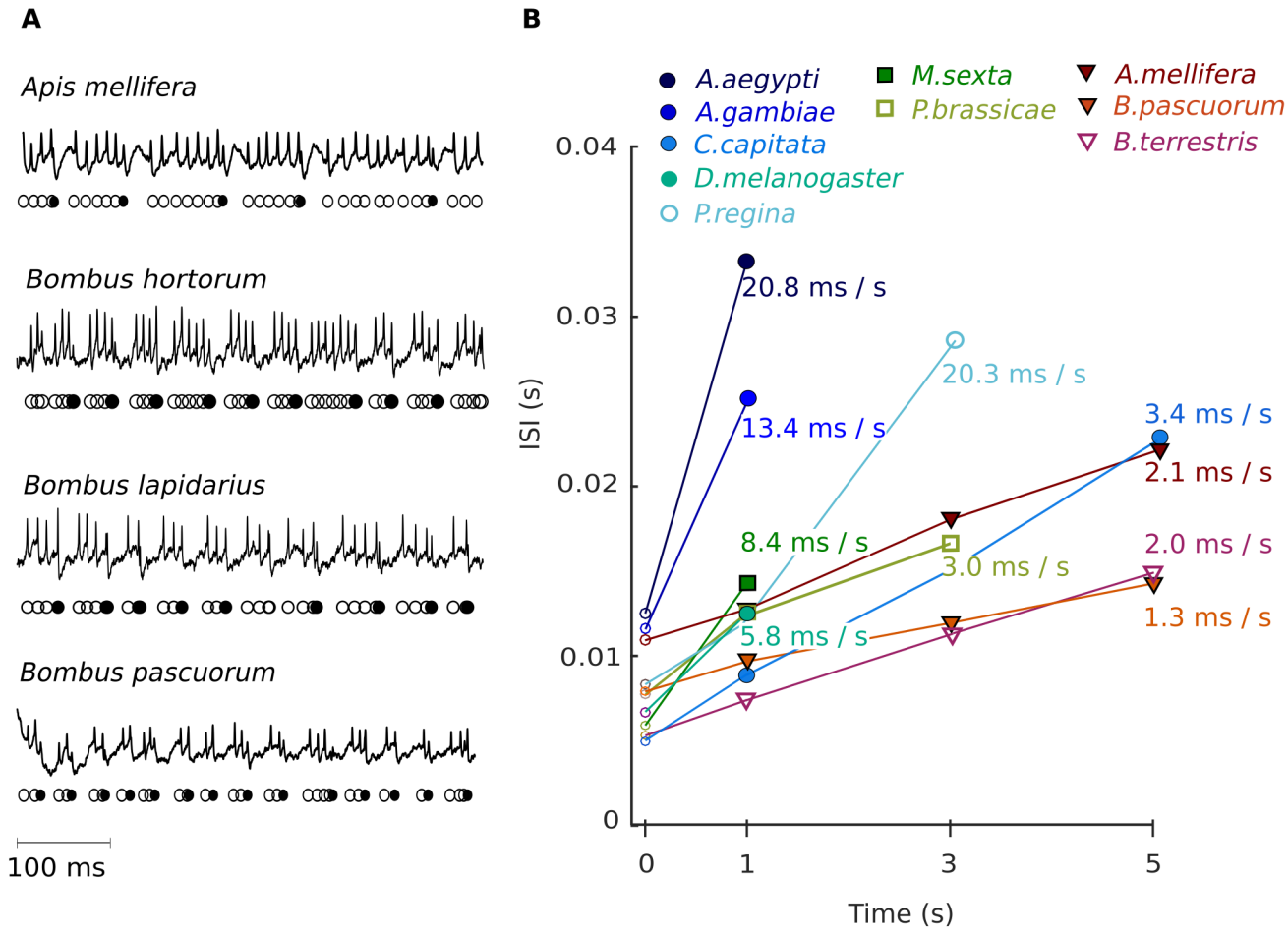
A
Apis mellifera
Bombus hortorum
Bombus lapidarius
Bombus pascuorum
100 ms
B
A.aegypti
A.gambiae
C.capitata
D.melanogaster
P.regina
M.sexta
P.brassicae
A.mellifera
B.pascuorum
B.terrestris
20.8 ms / s
13.4 ms / s
20.3 ms / s
3.4 ms / s
2.1 ms / s
8.4 ms / s
3.0 ms / s
2.0 ms / s
5.8 ms / s
1.3 ms / s
ISI (s)
0.04
0.03
0.02
0.01
0
0
1
3
5
Time (s)

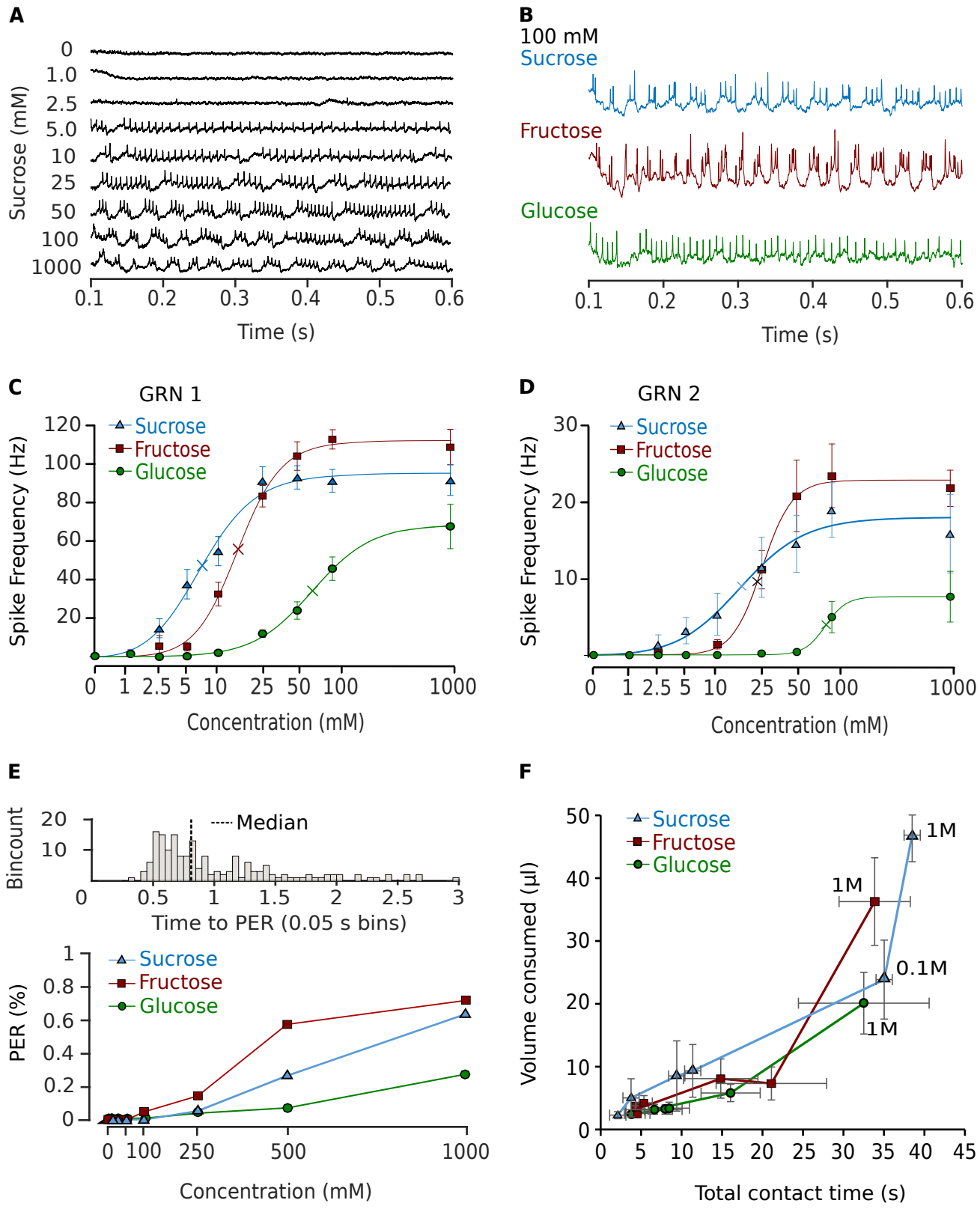
A
Sucrose (mM)
0
1.0
2.5
5.0
10
25
50
100
1000
0.1
0.2
0.3
0.4
0.5
0.6
Time (s)
B
100 mM
Sucrose
Fructose
Glucose
0.1
0.2
0.3
0.4
0.5
0.6
Time (s)
C
GRN 1
Sucrose
Fructose
Glucose
Spike Frequency (Hz)
120
100
80
60
40
20
0
1
2.5
5
10
25
50
100
1000
Concentration (mM)
D
GRN 2
Sucrose
Fructose
Glucose
Spike Frequency (Hz)
30
20
10
0
1
2.5
5
10
25
50
100
1000
Concentration (mM)
E
Bincount
20
10
0
0.5
1
1.5
2
2.5
3
Median
Time to PER (0.05 s bins)
Sucrose
Fructose
Glucose
PER (%)
1
0.8
0.6
0.4
0.2
0
0
100
250
500
1000
Concentration (mM)
F
Sucrose
Fructose
Glucose
Volume consumed (µl)
50
40
30
20
10
0
1M
1M
0.1M
1M
0
5
10
15
20
25
30
35
40
45
Total contact time (s)

Figure S1

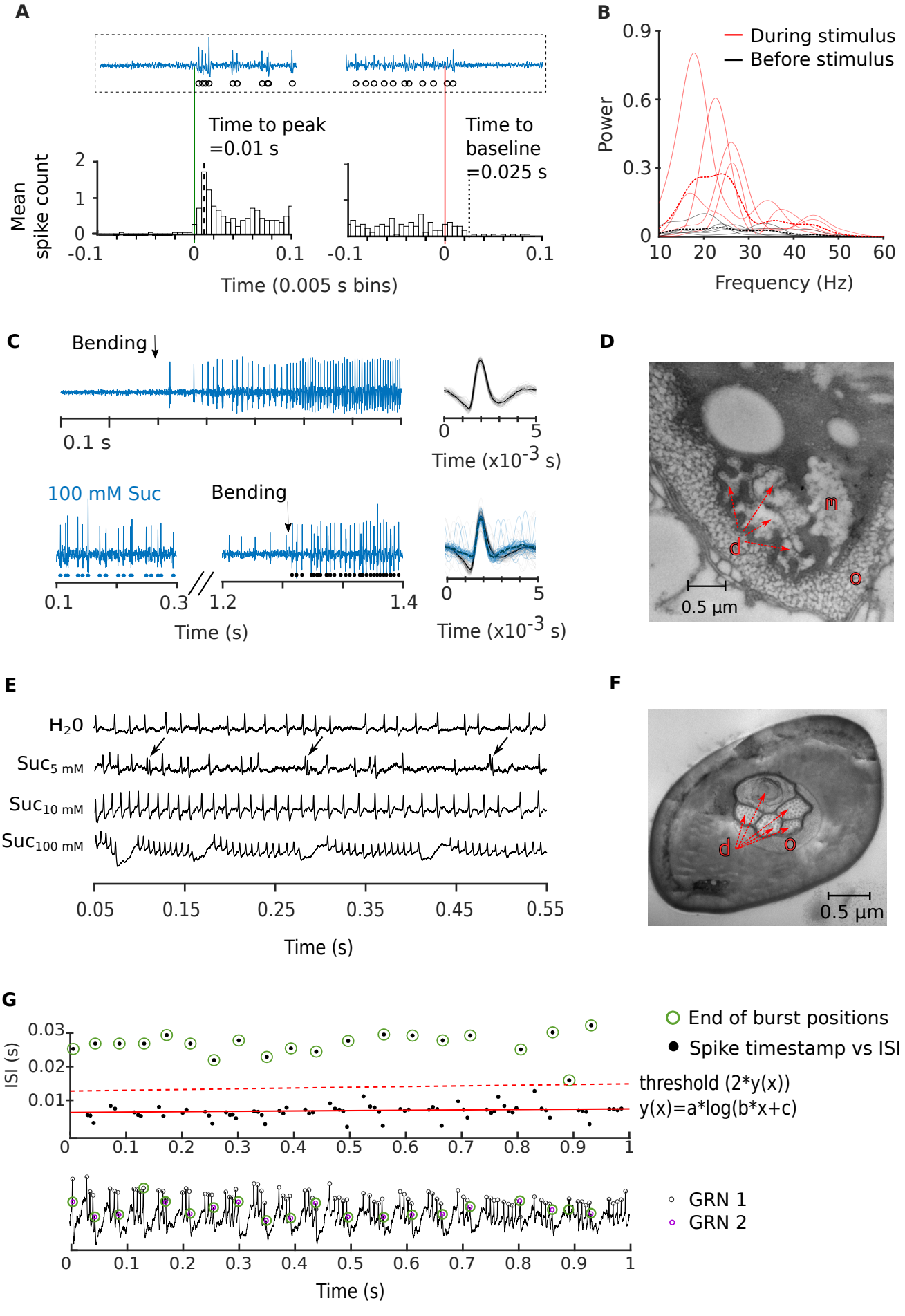
A
Time to peak
=0.01 s
Time to
baseline
=0.025 s
Mean
spike count
Time (0.005 s bins)
B
During stimulus
Before stimulus
Power
Frequency (Hz)
C
Bending
0.1 s
Time (x10-3 s)
100 mM Suc
Bending
Time (s)
Time (x10-3 s)
D
m
d
o
0.5 µm
E
H20
Suc5 mM
Suc10 mM
Suc100 mM
Time (s)
F
d
o
0.5 µm
G
End of burst positions
Spike timestamp vs ISI
threshold (2*y(x))
y(x)=a*log(b*x+c)
ISI (s)
GRN 1
GRN 2
Time (s)

Figure S2

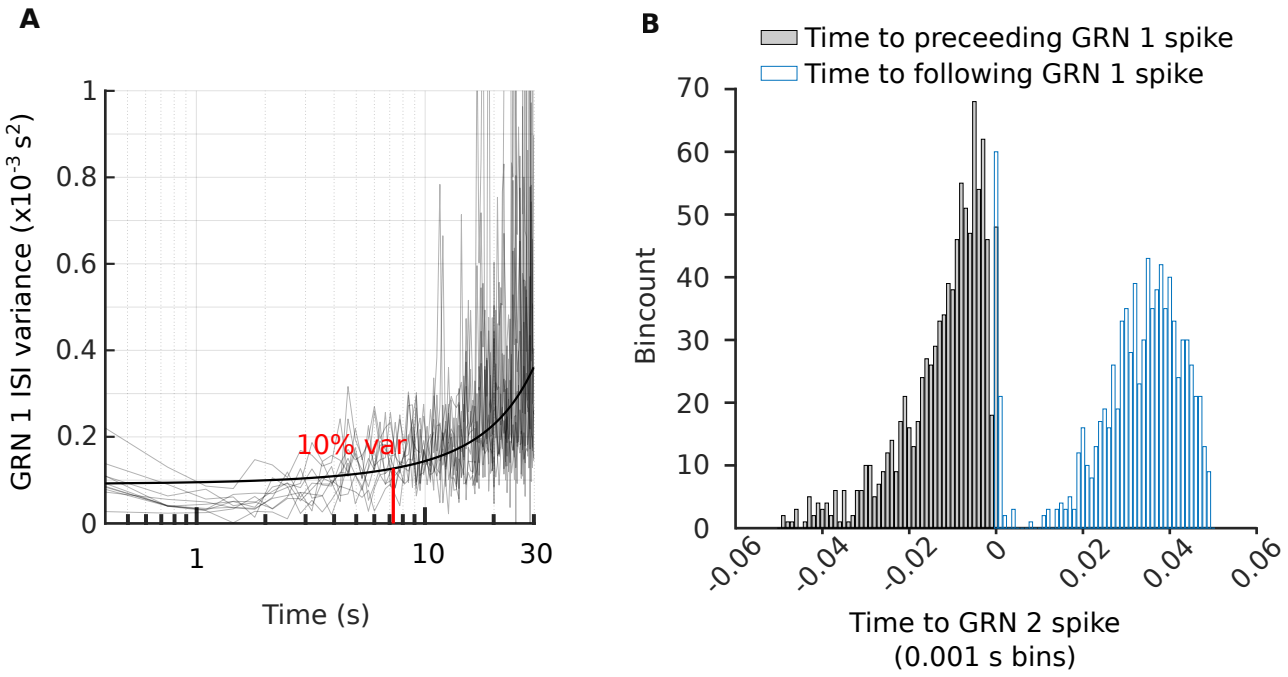
A
GRN 1 ISI variance (x10^{-3} s^2)
1
0.8
0.6
0.4
0.2
0
10% var
1
10
30
Time (s)
B
Time to preceeding GRN 1 spike
Time to following GRN 1 spike
Bincount
70
60
50
40
30
20
10
0
-0.06
-0.04
-0.02
0
0.02
0.04
0.06
Time to GRN 2 spike
(0.001 s bins)

Figure S3

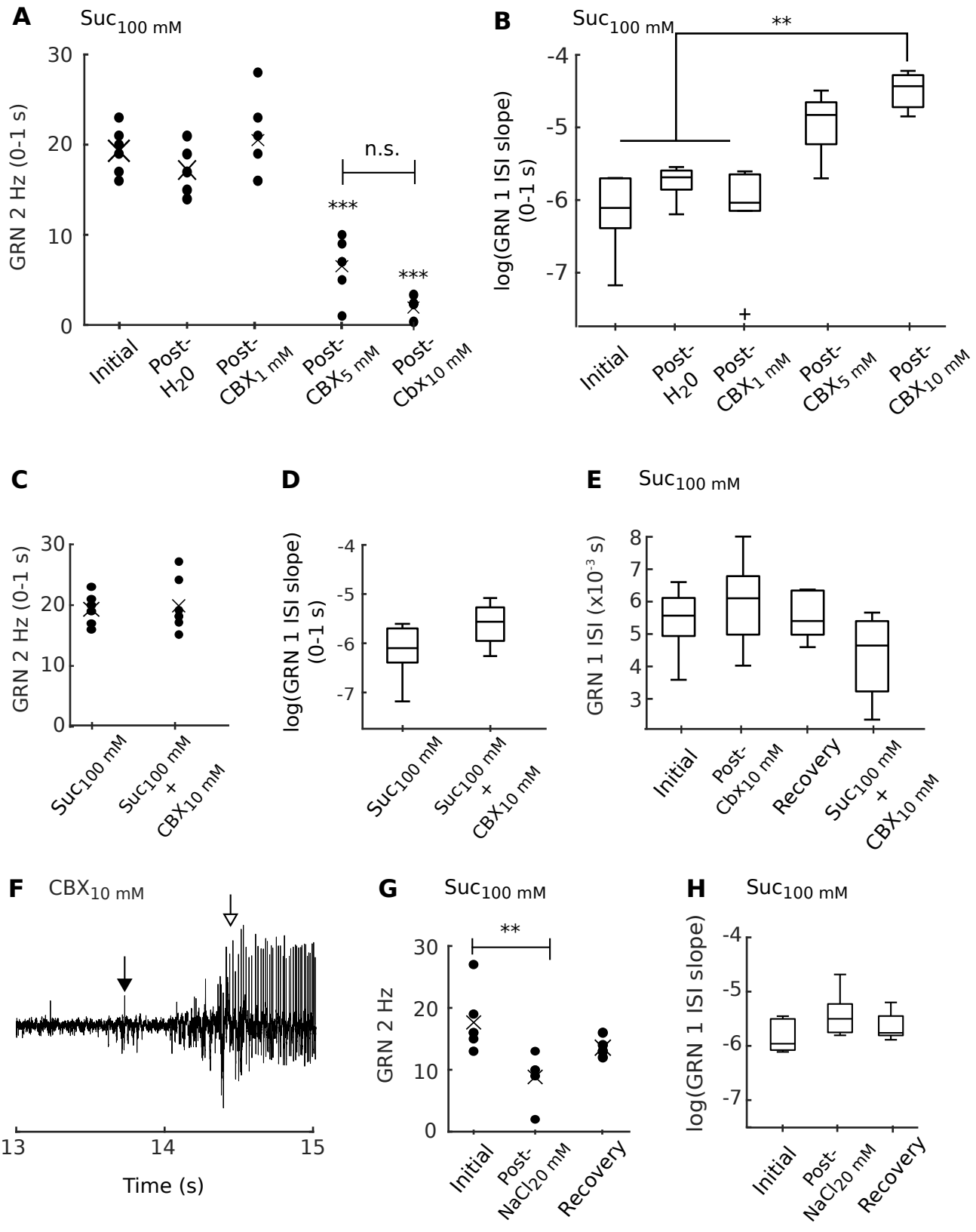
A
Suc100 mM
GRN 2 Hz (0-1 s)
n.s.
***
***
Initial
Post-H2O
Post-CBX1 mM
Post-CBX5 mM
Post-Cbx10 mM
B
Suc100 mM
**
log(GRN 1 ISI slope) (0-1 s)
Initial
Post-H2O
Post-CBX1 mM
Post-CBX5 mM
Post-CBX10 mM
C
GRN 2 Hz (0-1 s)
Suc100 mM
Suc100 mM + CBX10 mM
D
log(GRN 1 ISI slope) (0-1 s)
Suc100 mM
Suc100 mM + CBX10 mM
E
Suc100 mM
GRN 1 ISI (x10-3 s)
Initial
Post-Cbx10 mM
Recovery
Suc100 mM + CBX10 mM
F
CBX10 mM
Time (s)
G
Suc100 mM
**
GRN 2 Hz
Initial
Post-NaCl20 mM
Recovery
H
Suc100 mM
log(GRN 1 ISI slope)
Initial
Post-NaCl20 mM
Recovery

Figure S4

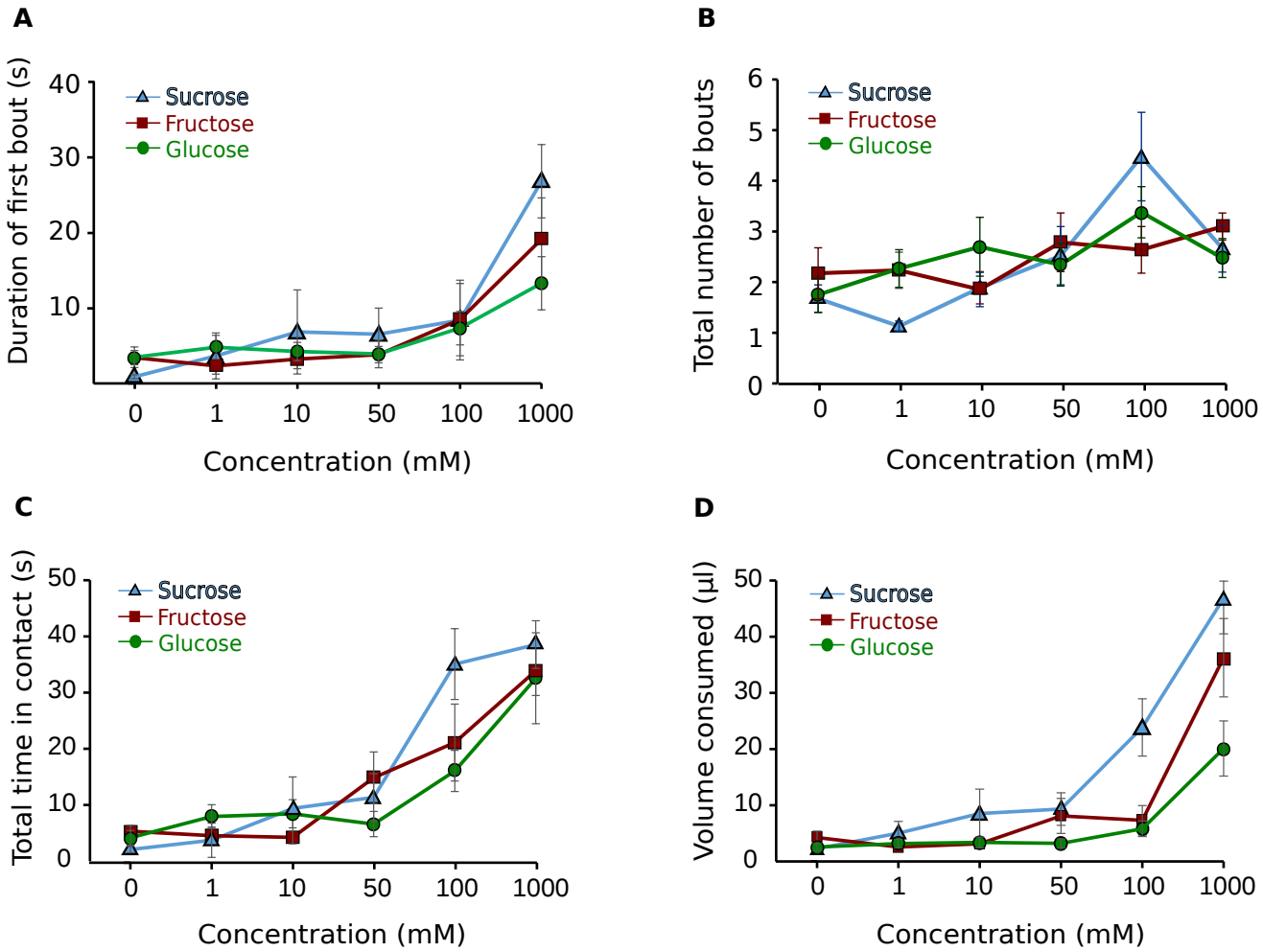
A
Duration of first bout (s)
40
30
20
10
Sucrose
Fructose
Glucose
0
1
10
50
100
1000
Concentration (mM)
B
Total number of bouts
6
5
4
3
2
1
0
Sucrose
Fructose
Glucose
0
1
10
50
100
1000
Concentration (mM)
C
Total time in contact (s)
50
40
30
20
10
0
Sucrose
Fructose
Glucose
0
1
10
50
100
1000
Concentration (mM)
D
Volume consumed (µl)
50
40
30
20
10
0
Sucrose
Fructose
Glucose
0
1
10
50
100
1000
Concentration (mM)

Supplementary figure legends

Figure S1: Stimulation with 100 mM sucrose activates two sugar-responsive GRNs, as shown in Figure 1. (A) Histogram of spike times (averaged over n=17 sensilla, 11 animals). On average, spiking starts 0.01 s from stimulus onset (green line) and stops within 0.025 s from stimulus offset (red line). Example 300-3000 Hz bandpass filtered tungsten recording is shown in inset. (B) Power spectral densities of the 10 -60 Hz frequencies (see Methods). The maximum power in this frequency range was significantly greater during stimulation (red traces) as compared to the baseline voltage before stimulation (black traces; 1-way ANOVA, $F_{2,12}$= 8.40, P < 0.001, n=5 recordings, 5 animals). Individual recordings shown as solid lines, averages as dashed lines. (C) **Top row**: Tungsten recording shows that the mechanoreceptor neuron is activated upon bending an A-type sensillum. Median spike waveform shown to the right. **Bottom row**: Bending the sensillum during 100 mM sucrose stimulation shows that the spike waveforms of the mechanoreceptor (black dots/waveform) are distinct from those of the sucrose responsive neurons (blue dots/waveform). Spikes were obtained from a 0.5 s duration after bending / stimulating with sucrose. (D) Transmission electron microscopy (TEM) at the base of an A-type sensillum shows the presence of four GRN dendrites (d) and a larger mechanoreceptor dendrite (m), encompassed by the outer lymphatic cavity (o). (E) Example tip recordings from a galeal B-type sensillum. The water-responsive GRN is active at 5 mM sucrose (as indicated by the presence of superpositions) but is inhibited at concentrations $\geq$ 10 mM sucrose. 100 mM sucrose evoked 106 ± 9 spikes/s and 8±3 bursts/s (mean±SEM, n=11 sensilla, 7 animals). (F) TEM at the base of a B-type sensillum shows the presence of 5 GRN dendrites. (G) Burst detection method. A three-term logarithmic equation ($y(x)=a*log(b*x+c)$; solid red line) was fit to the ISIs and their preceding spike timestamps (black dots). The fit used weights 1/ISI and robust least square regression. All spikes that were followed by an ISI greater than two times the fit (dashed red line) at the corresponding time point were considered as end of burst spikes (green circles). The corresponding spike sorted trace for this example is shown below. Since end of burst spikes are coincident with GRN 2 spike times, this burst detection method was used for estimating GRN 2 activity when spike sorting was not possible.

Figure S2: GRN 1 spike timing is correlated with spikes from GRN 2, see Figure 3. (A) Variance in ISIs per 0.3 s time bin for recordings with strong GRN 2 activity (>10 GRN 2 spikes in the first 1 s of stimulation; thin traces). An exponential equation ($a*exp^{b*x}$) fit over time shows that 10% of the maximum variance is reached after 7 s of stimulation (red line). (B) Histogram of ISIs preceding (grey) and following (blue) GRN 2 spikes shows that GRN 2 can be activated as long as 0.04 s after the preceding GRN 1 spike. GRN 1 spiking resumes around 0.03 s after the GRN 2 spike.

Figure S3. Exposure to the gap junction inhibitor carbenoxolone (CBX) suppresses bursting, as shown in Figure 4. A-B) Doses of CBX ≥ 5 mM CBX suppress bursting (i.e. GRN 2 spiking). (A) The number of GRN 2 spikes evoked in response to 100 mM sucrose stimulation decreased when sensilla were exposed to 5 mM and 10 mM CBX, but not 1 mM CBX or exposure to water, in comparison to the initial response to 100 mM sucrose (1-way ANOVA, $F_{4,27}$=41.2, ***P < 0.001). (B) Slopes of linear fits made to GRN 1 spikes over the first 1 s of stimulation. Only exposure to 10 mM CBX exhibits a significant increase in slope (i.e. a significant increase in rate of adaptation of GRN 1 spiking; 1-way ANOVA, $F_{4,27}$=13.8, ** P < 0.050). $4 \leq N \leq 5$ recordings per compound, 1 recording/animal. (C-D) Stimulating A-type sensilla with a solution of 10 mM CBX in 100 mM sucrose does not effect the number of GRN 2 spikes (C; 1-way ANOVA, $F_{1,12}$ = 0.04, P = 0.852) nor does it effect the GRN 1 ISI slope (D; 1-way ANOVA, $F_{1,12}$=4.10, P = 0.761, N=6 recordings, 1 recording/animal). (E) Exposure to 10 mM CBX, or stimulating with a solution of 10 mM CBX in 100 mM sucrose, does not effect the initial firing frequency of GRN 1 (N=5 sensilla, 5 animals, 1-way ANOVA $F_{3,24}$=2.30, P =0.103). Initial ISI (at time t=0 s) obtained from 3-term logarithmic fit made to GRN 1 ISI for

each stimulation. (F) Example segment of an extended recording shows that stimulation with 10 mM CBX evokes fluctuations in membrane potential (solid arrow). In 3 out of 7 recordings, the fluctuations lead to rapid spiking (open arrow) within 2 min of exposing the sensillum to 10 mM CBX. (G-H) As CBX is supplied as a disodium salt, we tested the effect of 20 mM NaCl as a control for the 10 mM CBX experiments. While stimulation with 100 mM sucrose after exposure to 20 mM NaCl does reduce the number of GRN 2 spikes in comparison to the initial 100 mM sucrose response, it is not significantly different from the recovery response (G; 1-way ANOVA, $F_{2,14}$=8.30,**P < 0.010). The GRN 1 ISI slope in the first 1 s of stimulation was not affected by 20 mM NaCl exposure (H; 1-way ANOVA, $F_{2,14}$=1.58, P = 0.246; N=5 animals, 1 recording/animal).

Figure S4: Bees feed longer and eat more on concentrations of sugars that produce bursting in GRNs, as shown in Figure 6. (A-C) The duration of the first feeding bout (A), the total number of bouts measured during the first 2 min of the feeding period (B) and the total duration of contact of the proboscis with the feeding solution (C) depended only on the sugar concentration but not of the sugar identity (see results and methods for statistical analyses). (D) The volume of solution consumed during the assay was a function of the sugar identity and the concentration (Gamma GLM with an inverse link function, effect of the concentration: F_6 = 47.5, P < 0.001, effect of the sugar identity, F_2 = 9.9, P < 0.001). Dataset used are same as in Figure 6 F.

Supplementary Tables

Legends:

Table S1. Slope values for 1 s segments of the curves fit in Figure 4D. A generalized linear model fit to the slope of 1 s intervals of a 5 s recording. P-values represent *post-hoc* pair-wise comparisons for the slopes of the 1st s of the recording compared to all other 1 s recording segments.

Table S2: Summary of the three-parameter (*a*,*b*, and *c*; see methods) log-logistic model for the GRN 1 spiking frequency (Hz; estimated as number of spikes in 1 s of recording) as a function of increasing concentration for stimulation as in Figure 6C. Fits were made individually for stimulation with fructose, sucrose and glucose stimulation. The t-statistics and corresponding p-values are for testing the null hypotheses that the parameters are equal to 0. All three parameters for the curve for each sugar are significantly different from 0 (all P < 0.05). The *a* parameter refers to the steepness of the model, the *b* parameter refers to the upper asymptote, the *c* parameter refers to the effective concentration at 50% (EC_{50}, the point at which the rate of firing reaches half of its maximum value). Pairwise comparisons for parameters ‘c’ and ‘b’ are included.

Table S3: Summary of the 3-parameters log-logistic model for the GRN 2 spike frequency as shown in Figure 6D (Hz; estimated as number of bursts in 1 s of recording) as a function of increasing concentration as in Table S2. Fits were made individually for stimulation with fructose, sucrose and glucose. Pairwise comparisons for parameters ‘c’ and ‘b’ are included.

Table S1

Generalized linear model			
	χ^2	**df**	**P-value**
Intercept	251	1	<0.001
Stimulus	62.5	2	<0.001
Interval	21.9	4	<0.001
Stim * interval	30.4	8	<0.001
Post-hoc comparisons			
Stimulus	**Interval**	**Mean slope**	**P-value**
Suc (initial)	0-1s	2.95	-
	0-1s vs. 1-2s	2.68	0.845
	0-1s vs. 2-3s	1.58	0.317
	0-1s vs. 3-4s	1.98	0.479
	0-1s vs. 4-5s	3.20	0.855
Post CBX	0-1s	11.52	-
	0-1s vs. 1-2s	6.13	<0.001
	0-1s vs. 2-3s	8.08	0.012
	0-1s vs. 3-4s	4.77	<0.001
	0-1s vs. 4-5s	3.20	<0.001
Suc (recovery)	0-1s	3.00	-
	0-1s vs. 1-2s	4.40	0.305
	0-1s vs. 2-3s	2.70	0.826
	0-1s vs. 3-4s	1.60	0.305
	0-1s vs. 4-5s	1.52	0.277

Table S2

Log-logistic model					
Sugar	**Parameter**	**Estimate**	**Std. error**	**t-value**	**P-value**
Fructose	a (steepness)	-2.2	0.3	-6.7	<0.000
	b (upper asymptote)	111.6	4.0	27.7	<0.000
	c (EC50)	15.2	1.4	11.1	<0.000
Sucrose	a	-1.7	0.2	-7.1	<0.000
	b	94.6	3.3	29.0	<0.000
	c	7.1	0.7	9.8	<0.000
Glucose	a	-1.7	0.5	-3.3	0.001
	b	68.4	7.1	9.7	<0.000
	c	67.8	13.7	5.0	<0.000
Pairwise comparisons					
Parameter c	**Comparison**	**Difference**	**Std. Error**	**t-value**	**P-value**
	Fructose - Glucose	-53	13.7	-3.8	<0.001
	Fructose - Sucrose	8.2	1.5	5.3	<0.001
	Glucose - Sucrose	60.7	13.7	4.4	<0.001
Pairwise comparisons					
Parameter b	**Comparison**	**Difference**	**Std. Error**	**t-value**	**P-value**
	Fructose - Glucose	43.1	8.1	5.3	<0.001
	Fructose - Sucrose	16.9	5.2	3.3	0.001
	Glucose - Sucrose	-26.2	7.8	-3.4	<0.001

Table S3

Log-logistic model					
Sugar	**Parameter**	**Estimate**	**Std. error**	**t-value**	**P-value**
Fructose	a (steepness)	-3.3	1.7	-2.0	0.050
	B (upper asymptote)	22.8	1.9	12.3	<0.000
	c (EC50)	25.2	3.4	7.5	<0.000
Sucrose	a	-1.5	0.5	-3.1	0.002
	b	17.9	2.0	8.9	<0.000
	c	16.6	5	3.3	0.001
Glucose	a	-4.9	10.7	-0.5	0.645
	b	7.6	3.0	2.5	0.012
	c	88.3	35.6	2.5	0.014
Pairwise comparisons					
	Comparison	**Difference**	**Std. Error**	**t-value**	**P-value**
	Fructose - Glucose	-63.0	35.7	1.8	0.079
	Fructose - Sucrose	8.6	6.0	1.4	0.152
	Glucose - Sucrose	71.7	36.0	2.0	0.048
Pairwise comparisons					
	Comparison	**Difference**	**Std. Error**	**t-value**	**P-value**
	Fructose - Glucose	15.2	3.5	4.3	<0.001
	Fructose - Sucrose	4.9	2.7	1.8	0.076
	Glucose - Sucrose	-10.3	3.6	-2.9	0.005